Detection of Collagen in Rat Abdominal Wound Healing: Contributions of Mesenchymal Stromal Cells and Platelet-Rich Plasma

by

Tanya Minteer

Submitted in Partial Fulfillment of the Requirements

for the Degree of

Master of Science

in the

Biological Sciences

Program

YOUNGSTOWN STATE UNIVERSITY

August, 2012

ETD Program

Digitally signed by ETD Program
DN: cn=ETD Program, o=Youngtown State University, ou=School of Graduate Studies and Research, email=etdadmin@cc.ysu.edu, c=US
Date: 2012.09.14 12:30:21 -04'00'

Detection of Collagen in Rat Abdominal Wound Healing:
Contributions of Mesenchymal Stromal Cells and Platelet-Rich Plasma

by

Tanya Minteer

I hereby release this thesis to the public. I understand this thesis will be made available from the Ohio LINK ETD Center and the Maag Library Circulation Desk for public access. I also authorize the University or other individuals to make copies of this thesis as needed for scholarly research.

Signature: _____
Tanya Minteer, Student Date

Approvals:

Signature: _____
Diana L.Fagan, Thesis Advisor Date

Signature: _____
Johanna Krontiris-Litowitz, Committee Member Date

Signature: _____
Mark D. Womble, Committee Member Date

Signature: _____
Peter J. Kasvinsky, Dean of School of Graduate Studies and Research Date

ABSTRACT

Although new surgical techniques and technologies have attempted to combat the occurrence of hernias, patients continue to suffer from hernias following abdominal surgeries. Regenerative therapy, including the use of bone marrow derived-mesenchymal stromal cells (MSCs) or platelet-rich plasma (PRP), offers a new avenue to reducing the problem of hernias seen in post-operative patients. In this study, midline laparotomies were performed on Lewis rats. The incision was repaired with CollaTape or Allomax mesh with or without the addition of MSCs and/or PRP. At 4 and 8 weeks postoperative, abdominal fascia was excised (n=7 per group). The current study attempted to detect collagen type I (COLI) with immunohistochemistry (IHC) in paraffin-embedded sections from CollaTape supplemented abdominal walls. IHC was unsuccessful at identifying COLI. Future studies may require the identification of new antibodies that are effective in paraffin-embedded tissues. Collagen amount and organization, and myocyte degeneration of healed abdominal walls repaired with AlloMax were compared using Trichrome stained slides. AlloMax, with the addition of MSCs, resulted in decreased collagen production when compared to AlloMax with PRP. However, abdominal wall repaired with AlloMax, PRP and MSCs had a greater positive correlation between collagen organization and amount than uninjured abdominal wall. MSCs ability to suppress immune response may be deleterious to abdominal wound healing when combined with Allomax surgical mesh. Although the use of MSCs did not improve collagen redistribution in a healing abdominal wound in this study, the research presented here may lead to future discoveries involving MSC supplemented wound repair.

Youngstown
STATE UNIVERSITY

One University Plaza, Youngstown, Ohio 44555
School of Graduate Studies and Research
330.941.3091
Fax 330.941.1580
graduateschool@cc.ysu.edu

Friday, January 29, 2010

Dr. Diana Fagan
Biology Department
UNIVERSITY

Re: IACUC Protocol # 02-09
Title: Autologous Mesenchymal Stem Cell Transplantation in Rats to Improve Fascial Repair

Dear Dr. Fagan:

The Institutional Animal Care and Use Committee of Youngstown State University has reviewed the aforementioned protocol you submitted for consideration titled **"Autologous Mesenchymal Stem Cell Transplantation in Rats to Improve Fascial Repair"** and determined it should be unconditionally approved for the period of **July 2, 2009** through its expiration date of **July 2, 2012.**

This protocol is approved for a period of three years; however, it must be updated yearly via the submission of an Annual Review-Request to Use Animals form. These Annual Review forms must be submitted to the IACUC at least thirty days ***prior*** to the protocol's yearly anniversary dates of July 2, 2010 and July 2, 2011. You must adhere to the procedures described in your approved request; any modification of your project must first be authorized by the Institutional Animal Care and Use Committee.

Sincerely,

Dr. Peter J. Kasvinsky
Associate Provost for Research
Dean School of Graduate Studies and Research

PJK:dka

C: Dr. Walter Horne, Consulting Veterinarian, NEOUCOM
Dr. Robert Leipheimer, Chair IACUC, Chair Biological Sciences
Dawn Amolsch, Animal Tech., Biological Sciences

ACKNOWLEDGEMENTS

I would like to thank my research advisor, Dr. Diana L. Fagan, for her support and advice while working on this research project. I also thank my committee members, Dr. Johanna Krontiris-Litowitz and Dr. Mark Womble, for their assistance. I'm truly grateful to Youngstown State University for the opportunities they have provided me. I would also like to acknowledge my family, especially Mom, for the open ears and words of encouragement during the frustrating times. Thank you all!

LIST OF FIGURES

	Page #
Figure 1: Tissue Press and Segmented Template	29
Figure 2: COLI Detection with Polyclonal Anti-Collagen I Antibody	40
Figure 3: Antibody and Fc Receptor Binding Diagram	41
Figure 4: Background Staining in Negative Control	48
Figure 5: Determining the Dilution for the Primary Antibody	54
Figure 6: Testing of a Sodium Citrate Antigen Retrieval Technique	58
Figure 7: Control Slide Stained with Masson's Trichrome	63
Figure 8: Experimental Slides Stained with Masson's Trichrome	64
Figure 9: Comparison of Collagen Organization between Groups	65
Figure 10: Comparison of Collagen Amount between Groups	66
Figure 11: Comparison of Myocyte Degeneration between Groups	67

LIST OF TABLES

	Page #
Table 1: Experimental Design	22
Table 2: Scoring Scale for Slides Stained with Immunohistochemistry	34
Table 3: Scoring Scale for Slides Stained with Masson's Trichrome	35
Table 4: Determination of Primary and Secondary Antibodies Dilutions	38
Table 5: Rat Serum as a Blocking Agent	43
Table 6: Testing of Hydrogen Peroxide Quenching of Endogenous Peroxidases	44
Table 7: Additional Quenching Methods	47
Table 8: New Preparation for Negative Controls Comparison	50
Table 9: AEC Ability to Stain Sections	51
Table 10: Antigen Retrieval by Microwave Method	53
Table 11: Heat Induced (75°C) Antigen Retrieval	56
Table 12: Heat Induced (95°C) Antigen Retrieval	57
Table 13: Testing Addition of DAB Enhancers	59
Table 14: Summary of Alterations to IHC Method	61
Table 15: Correlations of Scored Abdominal Wall Characteristics	70

LIST OF ABBREVIATIONS

ECM	Extracellular Matrix
IL	Interleukin
PDGF	Platelet-Derived Growth Factor
TGF-β	Transforming Growth Factor-Beta
VEGF	Vascular Endothelial Growth Factor
FGF	Fibroblast Growth Factor
EGF	Endothelial Growth Factor
PG	Prostaglandin
GM-CSF	Granulocyte Macrophage-Colony Stimulating Factor
MCP	Monocyte Chemoattractant Protein
CTGF	Connective Tissue Growth Factor
COL	Collagen
MMP	Matrix Metalloproteinase
PRP	Platelet-Rich Plasma
MSC	Mesenchymal Stem/Stromal Cell
DMSO	Dimethyl Sulfide
MEM	Modified Eagles Medium
EDTA	Ethylenediaminetetraacetic Acid
MEM	Modified Eagles Medium
α-Collagen I	Anti-Collagen I Polyclonal Antibody
IgG	Immunoglobulin G
α-Rat IgG	Biotinylated Anti-Rat IgG
α-Rat COLI	Anti-Rat Collagen Type I

α-Rat Myosin	Supernatant of Cell Line SC-71 – monoclonal antibodies against rat type 2A myosin heavy chain
FBS	Fetal Bovine Serum
AEC	Aminoethyl Carbazole
DAB	3, 3'-Diaminobenzidine Tetrahydrochloride
PBS	Phosphate Buffered Saline
IHC	Immunohistochemistry
NaAz	Sodium Azide
ELISA	Enzyme-Linked Immunosorbent Assay

TABLE OF CONTENTS

I.	Introduction	1-17
II.	Materials	18-20
III.	Methods	21-36
	a. Experimental Design	21
	b. Platelet-Rich Plasma Preparations	23
	c. MSC Collection	24
	d. MSC Culture	24-26
	e. Surgical Procedures	26-27
	f. Tissue Collection	27-28
	g. Immunohistochemistry	30-32
	h. Trichrome Staining	32-33
	i. Collagen Quantification	33-36
IV.	Results	37-69
	a. Immunohistochemistry of Paraffin-Embedded Tissues	37-60
	b. Effects of AlloMax Mesh on Wound Healing	62-69
V.	Discussion	71-84
VI.	References	85-97

Introduction

Approximately 9.8 million Americans will have some sort of abdominal surgery this year (DeFrances and Hall, 2007). Out of those incisions, as many as half will not heal properly. It has been estimated that there are more than 200,000 abdominal hernias repaired in the United States each year (DuBay *et al*., 2007; Franz *et al*., 2000). Not only can hernias cause severe pain but they significantly hinder prompt healing of a wound, leading to complications such as infections or consequential disease development. Hernias are an economic nuisance as well. Each hernia repair surgery and its respective recovery period may burden patients with lost wages and it forces the health care industry to spend more of their already limited budget (Franz *et al*., 2000). Furthermore, almost 50% of individuals experience recurrent hernias after their initial incident, therefore multiplying this problem with each recurrence (DuBay *et al*., 2007; Dubay *et al*., 2005; Klinge *et al*., 2001).

A hernia is a protrusion of an organ through the structure or muscle that usually contains it. Abdominal incisional hernias are a type of hernia that involves evagination through the abdominal wall after a patient has had an abdominal surgery. The abdominal wall is made of several layers. Skin is the outermost layer of the abdominal wall and while most research has focused on the healing properties of skin, disruption to this layer would not be the ultimate cause of abdominal herniation. Inferior to skin on the abdomen are the abdominal muscles sandwiched between two layers of fascia (Anurov *et al*., 2012). Damage to these layers of abdominal fascia and muscle could cause an increased risk of hernia formation. The peritoneum is the innermost layer of the abdominal wall

which lines the entire abdominal cavity and protects the organs within (Anurov *et al*., 2012).

It is necessary to understand the etiology of hernias before trying to address a solution to the problem. Once an abdominal incision is made, abdominal muscles are severely weakened. These affected abdominal muscles suffer from atrophy because their main insertion point, the linea alba, has been severed. Studies have also shown that abdominal muscles tend to retract laterally once a medial incision is made, which permanently decreases the transverse length of these abdominal muscles by at least 10% and causes a marked increase in wound tension upon suturing the incision closed (DuBay *et al*., 2007). Although the repair of abdominal muscle is important, the current research is also interested in the characteristics of healing abdominal fascia. The innermost fascial layer is the first layer of resistance to outward pressure of the organs and the outermost fascial layer helps maintain muscle integrity and wound closure. A sutured abdominal incision signifies the end of surgery but, more importantly, the beginning of the recovery process for the patient.

The body's wound healing process is very complex and involves numerous biological factors and processes. Variability in wound healing after abdominal surgery can affect the chances of herniation. If an abdominal incision repairs itself abnormally it can lead to weakened tissue in that area. Even when wounds heal properly, the resulting scar will only regain up to 80% of the strength of uninjured tissue (Franz *et al*., 2000; Stodtbeck, 2001). Patients often develop hernias after abdominal surgeries because their healed incision is weak and cannot resist the same pressures that it did before surgery

(Klinge *et al*., 2001; White *et al*., 2007). There are several theories surrounding the cause of weakened abdominal scar tissue which involve the wound healing process.

Wound healing is divided into four separate phases. The hemostasis phase begins the entire wound healing process. Next, the inflammatory phase continues the healing process which is then followed by proliferation and repair. The final stage of wound healing is the remodeling phase. Although each phase of wound healing serves a unique purpose, the mechanisms within the phases tend to overlap one another (Strodtbeck, 2001).

Hemostasis is defined as the stoppage of bleeding. This phase includes the formation of a clot, as well as vasoconstriction, and initiates the rebuilding of the extracellular matrix (ECM) (McCulloch and Kloth, 2010; Franz *et al*., 2000; Strodtbeck, 2001). Hemostasis begins at the moment of injury and is usually complete by three days post-injury. The first cytokine detected during the hemostasis phase is interleukin-1 (IL-1). IL-1 is released by leukocytes throughout the wound healing process, but more significantly, by keratinocytes, the most abundant epidermal cells, when the skin is wounded. The release of IL-1 initiates wound healing by signaling the injury to other cells nearby and causes the keratinocytes to proliferate and amplify their migration to the site of injury (Barrientos *et al*., 2008).

Because of the up-regulation of IL-1, platelets leave severed blood vessels within the dermis and rush to the injury site to begin clot formation (Ruggeri, 2002). Platelets then degranulate to release alpha and dense granules that contain several clotting proteins and growth factors. Among the substances secreted are serotonin, thromboplastin, and

fibrinogen, as well as platelet-derived growth factor (PDGF), transforming growth factor-beta (TGF-β), vascular endothelial growth factor (VEGF), fibroblast growth factor (FGF) and endothelial growth factor (EGF) (Strodtbeck, 2001; Barrientos *et al*., 2008; Ruggeri, 2002). The release of serotonin is responsible for vasoconstriction in this phase. Fibrinogen is converted into fibrin through the proteolytic action of thrombin found on the surface of platelets. Fibrin polymerizes to form the clot and provides a structure to which platelets and fibroblasts are attracted. The platelet-released growth factors activate fibroblasts which then make proteoglycans, glycosaminoglycans and, most importantly for this study, begin the synthesis of collagen. These molecules are all then integrated into the clot to begin the formation of a new ECM (Weisel *et al*., 1993).

Like the hemostasis phase, the inflammatory stage of wound healing starts with the initiation of skin injury but may last as long as one week. The inflammatory stage is important for initiating "clean-up" of the wound site by removing toxic components and damaged tissue. The characteristics of inflammation, such as redness, heat, and edema are a result of vasodilation and increased venule permeability at the site of injury. When the initial signal of trauma is received, the simultaneous release of histamine and serotonin from localized mast cells, kinins from α2-globulin in blood plasma, and the enzymatic breakdown of norepinephrine trigger the physiological events of inflammation. Without this initial signaling of the inflammatory phase, delivery of other essential cells, cytokines, and growth factors after this point would be hindered and could increase the healing time (Peacock, 1984).

Important mediators of inflammation are the prostaglandins, prostaglandin E1 and E2 (PGE1 and PGE2), secreted by white blood cells at the wound site. PGE1 is released

early in the inflammation phase to support vascular permeability, while PGE2 is released later in the inflammation phase and induces the migration of leukocytes to the wound site (Peacock, 1984). Additionally, the release of PDGF, IL-1, and granulocyte macrophage-colony stimulating factor (GM-CSF) calls inflammatory cells into the fibrous clot (Barrientos *et al*., 2008). Leukocytes pass through venule walls to the injury site by a process called diapedesis. Neutrophils and monocytes are the first leukocytes to migrate to the wound site, although neutrophils are more abundant. An abundance of this leukocyte is very important because neutrophils quickly begin eliminating foreign molecules within the wound by phagocytosis (Feng *et al*., 1998).

By the third day post-injury, neutrophils begin to undergo apoptosis (programmed cell death) while monocytes continue to migrate to the wounded area under the influence of various cytokines and chemokines, such as monocyte chemoattractant protein-1 (MCP-1) (Engelhardt *et al*., 1998). Platelets, keratinocytes, and fibroblasts, which are well established in the wound by this time, release TGF-β to initiate the conversion of monocytes into macrophages (Barrientos *et al*., 2008). Macrophages are able to control the rate at which a wound transitions from the inflammatory phase into the proliferation and repair phase. Not only are these phagocytes able to ingest bacteria and ECM debris that accumulates in the wound, but they are also an important source of cytokines and growth factors that are necessary to complete wound healing (Lang *et al*., 2002; Wahl, 1985; Barbul, 1990). Macrophages secrete PDGF which stimulates the enzyme collagenase to increase the elimination of damaged or old collagen in the wound. Fibroblasts respond to the PDGF signal and synthesize new collagen (Barrientos *et al*., 2008). Studies have shown that without macrophages, wounds would not be able to heal

correctly, but if they persist within a wound longer than normal, they can lengthen the healing time (Franz *et al*., 2000). Once the inflammatory phase has reached its goal of creating a clean wound site the process can continue into the third stage of proliferation and repair (Strodtbeck, 2001).

Under optimal conditions, the proliferation and repair phase of healing can be initiated as early as four days after injury. Wound environments become hypoxic once clotting occurs and this decrease in oxygen, combined with the presence of specific cytokines and growth factors, triggers angiogenesis and fibroblast proliferation. Fibroblasts are the primary active cells found within connective tissue from which the fibrous matrices are formed (Strodtbeck, 2001; Barrientos *et al*., 2008; Albina *et al*., 1995). Fibroblasts are first called to the injured site due to the increased concentrations of TGF-β, PDGF, FGF, and connective tissue growth factor (CTGF) which were secreted from macrophages, platelets and some endothelial cells during the earlier phases of wound healing. A large population of fibroblasts is needed to synthesize and replace collagen in the damaged ECM.

Angiogenesis, the formation of new blood vessels, contributes to the process of neovascularization associated with the repair phase. Neovascularization is best defined as the proliferation of these new blood vessels within the wound site to supply the area with increased oxygen and nutrients to ensure the quality of a healed wound. The accumulation of FGF that drew fibroblasts to the wound also accelerates the production of VEGF which then signals the proliferation and migration of endothelial cells during angiogenesis (Strodtbeck, 2001; Barrientos *et al*., 2008).

Another major occurrence in this third phase of wound healing is re-epithelialization. Re-epithelialization is initiated by CTGF, GM-CSF, EGF, FGF and TGF-β. The macrophages that accumulate during the inflammatory phase produce GM-CSF, EGF, and TGF-β. Mast cells which were involved in histamine secretion are also a source of FGF. The high number of fibroblasts now within the newly synthesized ECM releases CTGF when activated by TGF-β. While there are many sources of these re-epithelialization growth factors, they all target keratinocytes. When activated by these growth factors, keratinocytes migrate to the wound site, proliferate and undergo differentiation. Keratinocytes travel from uninjured tissue near the wound and adhere to the ECM of the injured area. Extraordinary conformational changes must take place in order for these keratinocytes to relocate. Keratinocytes must flatten to migrate and incorporate themselves into the wounded area assuming shapes similar to squamous cells (Strodtbeck, 2001; Barrientos *et al*., 2008; Marshall, 2004).

Keratinocytes can be found underneath the fibrin clot spanning the surface of a wound. The method in which they close the outer surface of the wound itself is quite complex. The now flattened cell stretches itself onto the dermal ECM, attaches temporarily and then contracts to move further across the wound opening. The process of "leapfrogging" occurs when a keratinocyte stops once it has moved only a few cell lengths across the dermal ECM and then other keratinocytes pass over this cell to complete the wound closure. Keratinocytes do not stop migrating across the wound's surface until contact is made between two keratinocytes that originated from uninjured skin at opposite ends of the wound. Once these epithelial cells terminate their migration, they form strong bonds with each other and the underlying basement membrane and then

reorganize to form the normal keratinocyte arrangement of uninjured skin (Strodtbeck, 2001; Ortonne *et al*., 1981).

Granulation tissue formation is the final event of the proliferation and repair phase. Granulation tissue is tissue that forms in place of the fibrin clot of the wound. This tissue is rich in collagen and blood vessels and usually is pink and moist in appearance. It is assembled by fibroblast activity beginning around four days after injury. As the fibrin in the clot of the wound is removed, new fibronectin, collagens and other ECM substances contribute to the development of the granulation tissue. Many elements are contained in the granulation tissue and contribute to its distinguishing visual characteristics. New blood vessels are responsible for its dark pink to red color and the lubricating glycoaminoglycan, hyaluronate, gives the tissue a moistened appearance. As the synthesis of granulation tissue continues, the fibroblasts involved begin to differentiate into myofibroblasts and clump together. With the help of actin and myosin in the myofibroblasts, the edges of the wound are contracted inward leaving a smaller wound opening. The proliferation and repair phase actively replenish the vasculature, epithelium and collagen in the wounded area for up to three weeks after injury (Strodtbeck, 2001; Tomasek *et al*., 2002).

New collagen is synthesized and distributed in amounts that vary from that of uninjured tissue (Strodtbeck, 2001; Ehrlich and Krummel, 1996). Although most research focuses on the collagen composition of skin, a comparative study suggested the proportions of collagen types within the fascia are slightly reduced but similar to skin collagen type ratios (White *et al*., 2007). The collagen composition of normal skin consists mainly of collagen type I (COLI). This collagen is usually the most abundant

and comprises about 80% of the dermis (Strodtbeck, 2001). Collagen type II (COLII) is also found in normal, uninjured skin but in smaller quantities that are often negligible (Junqueira *et al*., 1992). Collagen type III (COLIII) is commonly associated with COLI and makes up the remaining collagen (20%) network within normal skin (Strodtbeck, 2001). COLI forms thick fibers to resist the tension experienced at the wound site. Conversely, COLII and COLIII fibers are more loosely organized within their formed matrices and are less successful at resisting consistent, high tension (Junqueira *et al*., 1992). Fibroblasts make collagen types I, III and V during granulation. Before healing transitions into its final stage of remodeling, COLIII comprises an estimated 30% of the new ECM (Strodtbeck, 2001).

Replacement of connective tissue can cause the abdominal area to lose some of its pressure-resistant characteristics and the body is more prone to subsequent, tension-induced (stretching, bending or lifting) injuries at the site of healing which then becomes a potential site for hernias. Previous tensiometric studies have shown that the scar resulting from superficial healing causes the skin to become weaker and does not resist as much pressure as uninjured skin (DuBay *et al*., 2005). One reason for the weakness may be the breakdown of collagen by matrix metalloproteinases (MMPs). MMPs are responsible for the breakdown of specific collagen types and can be activated by neutrophils. There are many types of MMPs and each slightly varies in function. Most MMPs, like MMP-1 and MMP-13, can break down several types of collagen. MMP-1 and MMP-13 can both break down collagen types I, II, and III. Although MMP-13 is more capable of breaking down COLII than MMP-1, MMP-1 is more essential during wound healing (Vaalamo *et al*., 1997). Klinge *et al* examined the abundance of MMP-1

and MMP-13 in patients with abdominal hernias (Klinge *et al*., 2001). Their report stated that the presence of MMP-1 was significantly decreased and MMP-13 was completely eliminated within the fascia of hernia sufferers. The depletion of these MMPs led to a significantly decreased COLI/COLIII fiber type ratio of fascia from a hernia patient compared to normal, uninjured fascia. A decreased COLI/COLIII ratio is the result of an increase in COLIII fiber type and a decrease in COLI fiber type. While the specific contribution of rigidity or elasticity to the healed sites of each particular collagen type is still somewhat unclear, this study suggests the development of weaker fascia after abdominal herniation due to an unusually high amount of COLIII in this area (Klinge *et al*., 2001).

Finally, around three weeks post-wounding, the skin acquires scar tissue throughout the last phase of wound healing called tissue remodeling where old, original collagen at the wound site is broken down and replaced with a more organized distribution of new collagen fibers at the wound site. Macrophages that have been activated by PDGF are responsible for the up-regulation in MMPs which aid in degradation and removal of old, damaged collagen (Strodtbeck, 2001). New collagen continues to be produced by localized fibroblasts in response to TGF-β (Barrientos *et al*., 2008). While collagen is being replenished at a site of wounding there is also collagen degradation that occurs. The balance of these two processes affects the amount of new collagen formed within the healed site (Madden and Peacock, 1971).

Madden and Peacock found that there is a steady increase in the formation of new collagen during the first three weeks of healing but then collagen formation plateaus during the remodeling phase. However, the tensile strength of healing tissue increases

throughout the entire healing process. The data from Madden and Peacock's study suggests that collagen synthesis is greater than its degradation before entering the remodeling phase, but after this time the two processes equal each other. Results of this study also provided evidence that scar tissue will continue to gain strength throughout the duration of healing, even after the maximum collagen content has been reached (Madden and Peacock, 1971). The remodeling phase has long been known to be the only phase that focuses on the organization of collagen fibers. Before this phase, collagen fibers are produced and loosely placed within the repairing ECM. Remodeling can persist for several years until the healed skin achieves the maximum amount of strength possible. Healing skin achieves the majority of its tensile strength during the remodeling phase. Therefore, scars with highly organized collagen fibers would be expected to resist hernias better than scars with poorly organized collagen (Madden and Peacock, 1971).

The remodeling phase is mainly concerned with modifying the healing wound to mimic the attributes of uninjured skin as closely as possible. Throughout the first three phases of wound healing there is an increase in growth factors, cytokines, and cell types. The early cells that accumulate in the wound bed, such as macrophages, keratinocytes and fibroblasts, undergo apoptosis and consequently there is a decrease in growth factors and cytokines produced by them. The ECM does not gain additional collagen during remodeling; MMP activity may decrease the current amount of collagen to quantities less than uninjured tissue composition.

The physiological differences that have been identified in the composition of herniated tissue may be the result of a genetic disorder which impairs the maintenance of collagen. Although it is more evident in skin than in fascia, it has been suggested that

individuals with incisional hernias have reduced COLI/COLIII ratios before a laparotomy (White *et al*., 2007). In contrast, one review argues that weakened scar tissue is the result of poorly organized collagen fibers rather than a COLI/COLIII ratio decrease (Ehrlich and Krummel, 1996). This review reports that during the proliferation and repair phase granulation tissue has 10% more (a total of 30%) COLIII than uninjured skin, but once remodeling is in progress, MMPs specific for COLIII digest these collagen fibers leaving only a total of 10% of COLIII to make up the final scar's composition. However, all literature agrees that hernias develop because the scar that formed from the original surgical incision never reached its full strength potential during the remodeling phase. In order to combat this problem, modern techniques have been developed to either minimize the size of the area that is injured during surgery or to supplement the incision with additional strength during healing (Franz *et al*., 2000).

Endoscopy has made it possible to reduce the incision size needed to perform certain abdominal surgeries. Studies have proven that smaller wounds heal faster. By disrupting less of the natural skin as well, scars that form from incisions made for minimally invasive surgeries may be stronger than scar tissue of larger healed wounds (Dent, 1992). Our knowledge of the wound healing process has also aided in the design of new practices, such as priming or electrical field stimulation. These types of practices are used after surgery to decrease healing time. Priming is a procedure in which growth factors that normally are produced at the beginning of wound healing are applied to the incision after surgery to stimulate quicker wound closure (Smith *et al*., 2000). Electrical field stimulation is used to specifically hasten the remodeling phase (Kambic *et al*., 1993).

The use of surgical mesh is a new practice many surgeons now use following laparotomies (Zieren *et al*., 1999). Although the use of surgical mesh may only lengthen the time between hernia recurrences, it has been proven to decrease the recurrence of incisional hernias by approximately 50% (DuBay *et al*., 2007). There are several types of surgical meshes used for hernia repair. Some of the most popular mesh types are made of polypropylene, polyester, or polyglycolic acid. These mesh types can cause serious complications though by fusing with the surrounding musculo-fascial areas. Most frequently, bowel obstruction, infertility, and chronic pain and infection result from synthetic mesh adherence. The use of collagen matrices may serve as a better alternative to synthetic meshes because they do not cause the same post-surgical problems and retains the ability to improve abdominal wound healing and reduce the chance for hernia recurrence. These collagen matrices are derived from living sources to reduce graft rejection and are processed to remove any non-collagenous materials to obtain a homogenous product (Dufrane *et al*., 2008). The current study uses two varieties of collagen matrices, one that contains basement membrane and collagen components (Allomax) and one that is composed of only collagen (CollaTape). Additional substances may be applied to the mesh to improve the success of hernia repairs, including platelet-rich plasma (PRP) and stem cells.

Stem cells are a popular choice for regenerative research because of their unique and beneficial characteristics including self-rejuvenation. Stem cells have been reported as having either pluripotent or multipotent differentiating qualities. Pluripotent stem cells can be identified as true progenitor cells able to differentiate into any cell type of the body. Multipotent stem cells differentiate into one specific type of cell lineage such as

only cells of the mesoderm or ectoderm or only blood cells (Oreffo *et al*., 2005; Wagner and Ho, 2007, Han, 2005). Stem cells from the bone marrow may be either hematopoietic or mesenchymal. Mesenchymal stem cells (MSCs) are a type of multipotent stem cells of interest for the improvement of hernia repairs because they differentiate into cells of the mesoderm such as chondrocytes, myocytes, or fibroblasts. This is in contrast to hematopoietic stem cells which form new blood cells (Wagner and Ho, 2007).

There are many different sources for stem cells including adult circulating blood, umbilical cord blood, synovial membranes, and adult bone marrow from which MSCs may be isolated (Minguell *et al*., 2000). The availability and ease of culture of MSCs is another reason why they are attractive for clinical use. It is easy to culture MSCs *in vitro* because they are able to adhere to plastic, which is a readily available and inexpensive culture substrate (Javazon *et al*., 2001). Studies have also proven the immunosuppressive qualities of MSCs (Brinchmann, 2008). MSCs transplanted into a recipient will not stimulate an immune response and the host's body accepts them as "self" cells (Oreffo *et al*., 2005). The cells used in this study may be better classified as multipotent mesenchymal stromal cells due to the fact that they were cultured as heterogenous populations, but still are identified with the abbreviation MSCs. True MSCs would be cultured as a homogenous sample (Horwitz *et al*., 2005). The MSC cultures used in this study may also contain fibroblasts, marrow stromal cells, myoblasts, or adipocytes, but not hematopoietic cells.

Studies have shown that wounds mature to a final healed state much quicker with the addition of MSCs to the injured area (McFarlin *et al*., 2006). MSCs derived from the

bone marrow seem to provide the most success. This could potentially be explained by the hypothesis that endothelial progenitor cells of the skin originate from bone marrow and would be present in heterogenous cultures applied to wounds (Wang *et al*., 2007). MSCs derived from the synovial membrane and umbilical cord blood have also been studied and, while cells from these areas also provide sufficient healing of incisions, they are not the most favorable type of MSC. Synovial membrane-derived MSCs are not practical because they can completely deplete COLII in repaired sites and have a tendency to incorporate collagen type X, which should only be found in bone, into scar tissue (Dickhut *et al*., 2009). The use of fibroblasts instead of MSC applications during wound healing has also been tested, and although fibroblasts are efficient in repairing the connective tissue of disturbed skin while resisting ossification, they do not shorten the period of time it takes for a wound to heal (Yan and Yu, 2007).

PRP enhances healing because it provides wound sites with additional cytokines and growth factors normally found during natural wound healing. PRP is another common substance added to surgical mesh to enhance wound healing (Oreffo *et al*., 2005). Some of the more important and heavily studied growth factors found in PRP are EGF, FGF, TGF-β, PDGF, VEGF, CTGF and GM-CSF. These growth factors are all key stimulators for progression throughout the wound healing process (McFarlin *et al*., 2006). Many studies have also found that the use of PRP decreases the chance of infection and other subsequent problems by accelerating the wound healing process and shortening the time a wound is exposed to possible pathogens. Although many wounds healed better with PRP compared to naturally healed incisions, the strength of the healed PRP wounds were quite variable between individuals (Buchwald *et al*., 2008; Everts *et al*., 2006;

Saratzis *et al*., 2008). Supplying a fresh wound with a combination of PRP and MSCs may yield better healed surgical incisions at a more consistent rate. This question is addressed in the current study.

Mesh application of PRP with MSCs to a wound increases the level of growth factors found at the site of healing leading to a shorter healing time. Namely, FGF, TGF-β, VEGF and PDGF are the growth factors found at these sites in increased concentrations that aid in wound healing by inducing mechanisms similar to their known natural functions. TGF-β may be the most effective growth factor for improving wound healing (Han *et al*., 2005). Other growth factors, like VEGF and PDGF, increase MSC numbers and are also involved with collagen formation at the wound site (Marie *et al*., 2009). VEGF in particular is known to induce migration of white blood cells. Bone marrow-derived MSCs can produce VEGF levels up to twelve times higher than those found in normal healing tissue (Han *et al*., 2005).

In this study MSCs derived from bone marrow were used with a collagen lattice (CollaTape) or a human-derived acellular matrix (Allomax), along with the presence or absence of PRP, to assess the healing of abdominal incisions of rats. The abdominal incisions are first measured for the formation of new collagen using Masson's Trichrome stain. The specific types of collagen, namely types I and III, is to be distinguished by immunohistochemistry. The amounts of these collagen types identified within a MSC aided abdominal incision are then compared to abdominal incisions healing without MSC application and uninjured, abdominal wall. The classification and quantification of COLI is the main focus of this thesis. If successful, this research could provide a possible

solution to the current problem of hernia occurrence in patients recovering from abdominal surgeries.

Materials:

Animals

Rats for this study were male Lewis white rats (250-300g) purchased from Charles River Laboratories International Inc. (Wilmington, MA). Housing was provided by the animal care facility at Youngstown State University for at least one week before experimental use. The rats consumed standard rat chow and water ad libitum, and were monitored and cared for daily. Age-matched rats were used. The experimental protocol for this study was approved by the Institutional Animal Care and Use Committee at Youngstown State University.

Chemical and Media Supplies

Dimethyl sulfoxide, trypsin/EDTA and ethanols were produced by Sigma (St. Louis, MO). Penicillin, streptomycin, alpha-Modified Eagle's medium and Glutamax were supplied from Gibco (Grand Island, NY). Acetic acid, isopropanol, 47% formaldehyde solution, Hematoxylin, 29% ferric chloride, glacial acetic acid, 1% Biebrich scarlet aqueous solution, 1% acid fuchsin aqueous solution, phosphomolybdic acid, phosphotungstic acid, and aniline blue was supplied by Fisher Chemical Company (Fair Lawn, NJ). Fetal bovine serum (MSC qualified) was purchased from Invitrogen (Frederick, MD).

Surgical Supplies

Isoflurane was purchased from Vet One (Meridian, ID). Buprenorphine was bought from BenVue Laboratories, Incorporated (Bedford, OH). Allomax surgical mesh was provided by RTI Biologics, Incorporated (Alachua, FL). CollaTape was manufactured by Zimmer Dental (Carlsbad, CA). Vicryl sutures used were purchased from Ethicon (Somerville, NJ). The tissue press was fabricated for this study by Anthony Viviano of the Mechanical Engineering Department at Youngstown State University.

Immunohistochemical Supplies

Slides were prepared by Saint Elizabeth's Pathology Department. Xylene was purchased from J.T. Baker (Phillipsburg, NJ). Hydrogen peroxide was manufactured by TopCare (Skokie, IL). The protein blocking agent was manufactured by Immunon (Pittsburgh, PA). Sodium citrate was supplied from Mallinckrodt (Paris, KY). The primary antibodies used in this study were polyclonal anti-collagen I antibody (α-Collagen I) purchased from Thermo Scientific (Rockford, IL), biotinylated anti-rat immunoglobulin G (α-Rat IgG) from Vector Laboratories (Burlingame, CA), anti-rat collagen type I (α-Rat COLI) from Millipore (Temecula, CA), and the supernatant of cell line SC-71 (α-Rat Myosin) from American Type Culture Collection (Manassas, VA). The secondary antibody used was biotinylated goat anti-rabbit IgG. The biotinylated goat anti-rabbit IgG secondary antibody, streptavidin-horseradish peroxidase conjugates solution, ClearMount mounting solution, aminoethyl carbazole and 3, 3'-diaminobenzidine tetrahydrochloride substrate solutions were purchased from Invitrogen

(Frederick, MD). The mounting solution used in this study was Shandon xylene substitute mountant from Thermo Scientific (Pittsburgh, PA).

Methods:

Experimental Design

In the current study, 7 groups of Lewis rats (n=14) underwent surgery where each rat received a single abdominal incision. The incision of each group was closed slightly different depending on the mesh or regenerative agents used to repair the abdominal wall. CollaTape or AlloMax were the mesh materials used to repair rats. CollaTape is a porous wound dressing made of purified type I bovine collagen. AlloMax is an acellular sterile surgical graft material processed from human dermis. Rats of Groups 2, 3 and 4 (**Table 1**) had CollaTape sutured into their abdominal wall during laparotomy closure. Group 2 rats had 0.5 ml of platelet-rich plasma (PRP) applied to the CollaTape. Group 3 received a mesenchymal stromal cell (MSC)/PRP mixture which was prepared with frozen MSCs applied to the CollaTape. Group 4 had the MSC/PRP mixture that was prepared with fresh MSCs applied to the CollaTape. Groups 5, 6, 7, and 8 had Allomax secured over their abdominal wall incision. Group 5 received Allomax with PRP and fresh MSCs. Group 6 rats had PRP only. Group 7 had 1 x 10^6 fresh MSCs applied to the Allomax with no PRP. Group 8 rats received Allomax alone (without MSCs or PRP). The abdominal wall was excised at 4 and 8 weeks post-operative (n=7 per group). Tissue excised at 4 weeks was designated as subgroup "a" for each group and tissue excised at 8 weeks was designated as subgroup "b" for each group. Control subjects did not receive a laparatomy but all rats of the control group had their abdominal wall excised at the same time as rats of subgroup “b”.

Table 1. Experimental Design

Group Name	Mesh Material Used[a]	Regenerative Agent Applied[b]	Postoperative Time Until Fascia Excision
Control	None	None	8 weeks
2a	CollaTape	PRP only	4 weeks
2b	CollaTape	PRP only	8 weeks
3a	CollaTape	PRP + frozen MSCs	4 weeks
3b	CollaTape	PRP + frozen MSCs	8 weeks
4a	CollaTape	PRP + fresh MSCs	4 weeks
4b	CollaTape	PRP + fresh MSCs	8 weeks
5a	AlloMax	PRP + fresh MSCs	4 weeks
5b	AlloMax	PRP + fresh MSCs	8 weeks
6a	AlloMax	PRP only	4 weeks
6b	AlloMax	PRP only	8 weeks
7a	AlloMax	Fresh MSCs only	4 weeks
7b	AlloMax	Fresh MSCs only	8 weeks
8a	AlloMax	None	4 weeks
8b	AlloMax	None	8 weeks

[a] Rats, except for the control group, received a 6 cm incision along the ventral midline severing the abdominal wall through the peritoneum. After fascia was closed, a mesh material was sutured to the anterior sheath.

[b] Regenerative agents were applied to the CollaTape mesh following its attachment to the anterior sheath.

Platelet-Rich Plasma Preparation

A 10mL syringe with a 21 gauge needle was prepared with anticoagulant citrate dextrose at a ratio of 1/10. The needle was placed intracardially in an anesthetized male Lewis rat (250-300g) to obtain 5-10 milliliters of blood. This blood was centrifuged at 200 X *g* for 10 minutes at 23°C. The plasma portion of the resulting centrifuged blood was removed and centrifuged at 700 X *g* for 10 minutes. The resultant platelet poor plasma supernatant was removed (with the exception of one milliliter) and stored at -20°C. Dimethyl sulfide (DMSO) (5%) was added to the remaining platelet pellet. The platelet pellet was resuspended and placed in a cryovial and the temperature was slowly reduced to -80°C. Frozen platelet suspensions were stored in liquid nitrogen.

When PRP was needed, the platelet poor plasma was brought to 37°C and one milliliter of the thawed platelet poor plasma was placed in another centrifuge tube. The frozen platelet pellet was thawed to the point where it dislodged and was added to the centrifuge tube containing the one milliliter of platelet poor plasma. The ice pellet was thawed quickly in the plasma by mixing in a conical tube. The tube was then centrifuged at 700 X *g* for 10 minutes at 4°C. After centrifugation, the top layer of plasma was discarded. The remaining platelet pellet was resuspended in the remaining platelet poor plasma. The final PRP mixture was administered to each incision at 0.5 milliliters per incision.

MSC Collection

To isolate bone marrow stem cells, bone marrow was harvested from the bones of donor rats. Rats were euthanized by performing a pneumothorax while under isoflurane (3-5%) inhalation anesthesia. For a sterile surface, a paper towel that was previously immersed in 70% ethanol was laid flat on a dissection tray. The rat was laid on the ethanol soaked paper towel and their fur was saturated with 70% ethanol. Scissors and rat tooth forceps were sterilized by coating their cutting surfaces with 95% ethanol and passing them quickly through a flame. The scissors were used to make an inguinal incision in the loose skin. The resultant flaps of skin were pinned to each side. Ethanol (70%) was poured over the surgical site to remove debris.

The subject's legs were removed by holding the hind legs with the rat tooth forceps and using the scissors to remove muscle tissue from the leg bones. The legs were then removed from the animal at the hip joint and the feet were subsequently removed. Epiphyses of the long bones were kept undisturbed during the limb removals. Each pair of detached legs was placed in a culture dish on ice with serum free alpha-Modified Eagles Media (αMEM). The tibia and femur were separated with scissors. The bones were transferred to sterile media under the cell culture hood.

MSC Culture

The following procedure was performed using sterile technique in a laminar flow hood. The epiphyses of the tibia and femur were removed and a 21 gauge needle attached to a syringe was inserted into each end of the leg bones. Alpha-MEM media

without fetal bovine serum (FBS) was flushed through the center of the bones to collect marrow in a petri dish. To produce a single-cell suspension, bone marrow was drawn in and out of the syringe through the needle and transferred to a 12 ml conical tube. The conical tube was allowed to sit for 4 minutes until clumps settled. The supernatant was then transferred to a new conical tube and a sample of this was taken and mixed with 4% acetic acid to lyse red blood cells and a cell count was obtained using a hemacytometer. The sample was then centrifuged at 600 X g for 8 minutes at 4°C. Cells were resuspended in complete stem cell media warmed to 37°C at a concentration of 10^5 – 10^6 cells/ml. This complete stem cell media contained αMEM, 20% MSC qualified FBS, 1mM Glutamax, 100U/ml of penicillin, and 100 µg/ml streptomycin. Glutamax is used as a replacement media for L-glutamine, which reduces ammonia concentrations in media during cell culture.

The cells were then deposited in a T75 culture flask. The flask was incubated for 4 days at 37°C with 5% CO_2. At day 4, any non-adherent cells were aspirated off. The media was replaced twice a week. Once growth reached 80% confluency, phosphate buffered saline (PBS) was used to wash the flasks. To release adherent cells (MSC suspension), the flasks had 3 ml of 0.25% trypsin/1.0mM EDTA added to it which was previously warmed to 37°C. When the cells rounded up, the cells were dislodged by tapping the flask. The cells were resuspended in media and the recovered cells were distributed into 2 new flasks. The culture process was repeated until cells had been passed three times. The final collection of MSCs (after 3 passes) was centrifuged at 600 X g. The pellet was resuspended and cells were counted. MSCs (10^6 cells/ml) were frozen in complete stem cell media containing 10% DMSO. Freezing was accomplished

by decreasing the temperature slowly to -80°C. The frozen cells were stored in liquid nitrogen.

MSCs designated as fresh MSCs in this study were thawed from frozen stock and cultured overnight in complete stem cell media at 37°C with 5% CO_2 prior to use. Fresh MSCs were released from the plate by incubation in trypsin/EDTA and counted using a hemacytometer. MSCs designated as frozen MSCs in this study were thawed from frozen stock and not cultured overnight before use. Each dose of MSC/PRP mixture contained 1 x 10^6 MSCs suspended in 0.5 ml of PRP and stored in a syringe on ice until application.

Surgical Procedures

Sterile technique was used during surgical procedures. Instruments were autoclaved or sterilized in a dry sterilization unit before surgery and between surgeries these instruments were cleaned with 70% ethanol, towel dried and placed in a hot bead sterilizer for re-sterilization.

Isoflurane inhalation was used as the method of anesthesia for all rats. Rats were exposed to a higher dose of 3-5% isoflurane initially in a polycarbonate induction chamber and then were moved to a surgical bed with a reduced amount of isoflurane (1-3%) to maintain sedation through a fitted nose cone. The rats were subcutaneously injected with 200 µl of buprenorphine analgesic (0.03 mg/ml) prior to surgery. The abdomen was prepared for surgery by shaving the area, scrubbing with betadine and rinsing with 70% isopropanol. The maximum amount of time any one rat spent under

anesthesia was 40 minutes. The rat's physical state was checked throughout surgery by monitoring respiration rates, tissue color, and toe pinch reflex.

To produce a wound healing site, a 6 centimeter incision was made along the linea alba of the abdomen through to the peritoneum. The fascia was closed with 5-0 Vicryl sutures in a running stitch pattern. A 6 x 1 cm strip of repair mesh was attached to the anterior rectus sheath with 6 individual 5-0 Vicryl sutures at the 4 corners and halfway down the length of the tape. To ensure MSCs adhered to the Allomax mesh, the fresh MSCs were applied to Allomax strips and incubated overnight before the mesh was surgically implanted into the rat. For the groups receiving PRP, the PRP was applied to the Allomax after placement over the sutured fascia. Skin was sutured with single 5-0 Vicryl subcuticular sutures. All subjects received subcutaneous injections of buprenorphine (0.03 mg/kg) 12 and 24 hours post-operative. During the week following surgery, rats were observed once daily to check for infection at the wound site.

Tissue Collection

The abdominal test areas were collected by first euthanizing a rat by isofluorane inhalation followed by blood collection through cardiac puncture and performing a pneumothorax to ensure expiration of the rat. The cardiac blood was used for PRP preparations. The skin was cut along the midline and folded back to expose the test area (muscle and fascial layers). Transverse incisions were made in the muscle layer through to the peritoneum above and below the original midline incision. These transverse cuts made it possible to slide a stainless steel plate under the test area. The steel plate was

held on a support and the test area was sectioned into 5 segments with a tissue press. **Figure 1** shows the tissue press and template used to cut the 5 segments from the rat abdominal wall. One of these segments, the most posterior, was added to 10% formalin in saline and sent to Saint Elizabeth's Hospital for microscope slide preparation. Tissues were paraffin embedded and 5 micron sections were placed on slides. One slide from each sample was stained with Masson's Trichrome for total collagen detection. One other slide from each sample was stained with Hematoxylin and Eosin for analysis of tissue morphology.

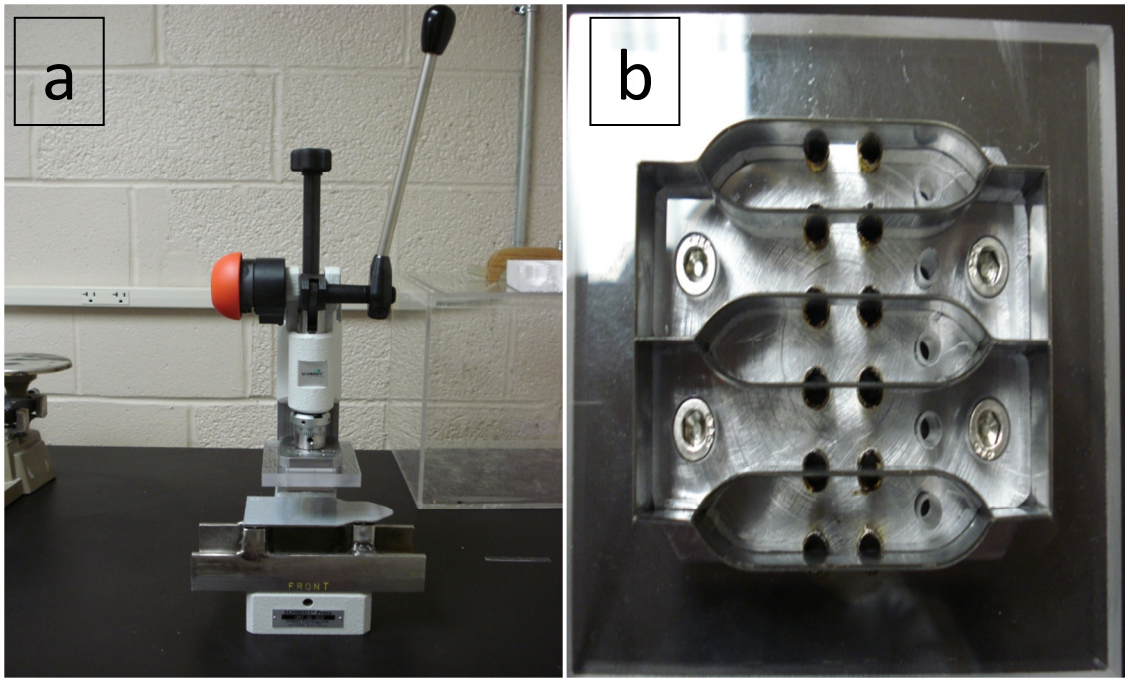

Figure 1. Tissue Press and Segmented Template: Tissue press (a) and template (b) used during tissue collection to uniformly cut the 5 test sections of the rat abdominal wall.

Immunohistochemistry (IHC)

Slides made from the abdominal tissue of rats repaired with CollaTape were baked on a heating block at 60°C for 2 hours and allowed to cool at 23°C overnight to assure the adherence of tissue sections to the slides. This pre-baking procedure was omitted for some staining procedures. Slides that were pre-baked are noted. Paraffin was melted on slides by heating them for 15 minutes at 60°C. Slides were then passed through 3 different xylene baths for 7 minutes each to deparaffinize sections. Slides entered a series of alcohol baths (100, 100, 95, 70, 50%) for 1 minute each in order to hydrate the samples. After hydration of the samples, they were rinsed in distilled water and PBS sequentially for 5 minutes each. Tissues were incubated in a 23°C humidified chamber with 0.03% (Caldwell *et al*., 2005), 0.3% (Li *et al*., 1987) or 2.7% H_2O_2 diluted in PBS for 15-20 minutes to inactivate endogenous peroxidases. The slides were rinsed with a wash bottle of PBS and set in a stirring PBS bath for 10 minutes. Protein blocking agent was applied to the slides for 20 minutes to prevent non-specific staining and then slides were incubated in 100-150 µl of PBS diluted primary rabbit antibody directed against human collagen type I (α-Collagen I), rat immunoglobulin G (α-Rat IgG), rat collagen type I (α-Rat COLI) or rat type 2A myosin heavy chain (α-Rat Myosin) for 1 hour. After incubation, the slides were rinsed in a stirring PBS bath again for 10 minutes. Using biotinylated anti-rabbit immunoglobulin in PBS, slides were incubated for 20 minutes in a humidified chamber at 23°C. The slides were rinsed again, and re-submerged into the PBS stirring bath for 10 minutes. A streptavidin-horseradish peroxidase conjugate diluted to 0.1 µg/ml with PBS was applied to the slides and incubated for 20 minutes inside the humidified chamber at 23°C. The slides were once

again rinsed and placed in a PBS stirring bath for 10 minutes. Slides were finally incubated with 100 µl of 3, 3'-diaminobenzidine tetrahydrochloride (DAB) or aminoethyl carbazole (AEC) solution until a color change was noticed in the tissue. Enhanced DAB solutions were tested, as well, to intensify staining. For these enhanced DAB solutions, DAB was mixed according to manufacturer's instructions and had 50 µl of the kit's enhancer, 0.0013M cobalt chloride, 0.01M imidazole, or 0.05% nickel chloride added to it (Werner *et al*., 1996). Slides were washed with tap water for 5 minutes. A dehydration series of ethanols were used on tissues for 1 minute per bath. The baths included a 50% bath, 70% bath, 95% bath and two 100% baths. Dehydration was followed by a one minute pass through a xylene bath to clear slides before mounting. If AEC was used as the colorimetric substrate, dehydration was not performed on the slides and 100-150 µl of ClearMount was dropped onto the tissue and slides were baked for 30 minutes on a 60°C heating block or until the ClearMount was dry. Shandon's non-aqueous, xylene substituted mounting material was used to mount all slides.

A negative control was created for each staining procedure by replacing the primary antibody incubation with PBS incubation. Antigen retrieval with a heated citrate buffer method was recommended for optimal antigen detection with α-Rat COLI antibody. Any procedure involving this antibody included heating of a 0.01M sodium citrate buffer by way of microwave or water bath. Antigen retrieval was always performed after the H_2O_2 incubation step. The microwave method was performed by immersing slides into a pre-heated 95°C sodium citrate buffer for 2 minutes and then 30 second heating intervals for duration of 5 minutes. The water bath method pre-heated the

sodium citrate buffer to either 75°C or 95°C and slides were immersed in the heated buffer for 10, 20 or 30 minutes.

Trichrome Staining

A trichrome staining method was performed to histologically distinguish collagenous areas of the tissue sections taken from rats repaired with AlloMax (Carson, 1997). Sections were deparaffinized followed by rehydration in distilled water. Slides were then left in a bath of Weigert Hematoxylin for 10 minutes. Initial solutions of 1% Hematoxylin made in 95% alcohol and 29% ferric chloride aqueous solution diluted by a factor of 25 with 1% glacial acetic acid were added to each other in equal parts to make the Weigert Hematoxylin. Slides were washed for 10 minutes in a running water bath followed by a rinse in distilled water. Next, slides were subjected to a 2 minute Biebrich scarlet-acid fuchsin solution (360 ml of 1% Biebrich scarlet aqueous solution + 40 ml of 1% acid fuchsin aqueous solution + 4 ml of glacial acetic acid) bath and rinsed with distilled water. Slides were placed in a phosphomolybdic/phosphotungstic acid bath for 10-15 minutes. Phosphomolybdic/phosphotungstic solution was made of 25g of phosphomolybdic acid, 25g of phosphotungstic acid, and 1L of distilled water. After being rinsed with distilled water, slides were transferred to an aniline blue bath for 5 minutes. This aniline blue solution was made of 25g of aniline blue mixed in 20 ml of glacial acetic acid and 1L of distilled water. Slides were again rinsed with distilled water. Slides were left in a 1% acetic acid bath for 3-5 minutes. The sections were dehydrated

with 2 baths of 95% ethanol and 2 baths of 100% ethanol. Each alcohol bath was for 1 minute. Slides were cleared with 2-3 baths of xylene for 1 minute each and mounted.

Collagen Quantification

Intensity of color on IHC stained slides (CollaTape supplemented abdominal wall) was grossly examined with a light microscope at 40x total magnification by 2 observers. IHC staining was scored on a scale from 0-4 based on the intensity of the resultant stain. A score of 0 indicated no staining and 4 indicated the most intense color observed. **Table 2** indicates the scale used for scoring IHC stained slides.

Photographs of the incisional areas were taken for trichrome stained slides at 100x and organized into a slide show. Total collagen was identified by blue staining while muscle stained red. The histological images were scored by 2 blinded investigators for collagen abundance, collagen organization and myocyte degeneration. A scale of 0-3 was used to score each characteristic. A score of 0 was given for samples with no collagen, disorganized collagen fibers or no myocyte degeneration. A score of 3 indicated abundant total collagen or myocyte degeneration and well organized fibers. Organized collagen fibers were identified as having parallel orientation and no separations between strands, while disorganized collagen was found in random orientations and interspersed between fat and muscle tissue. Myocyte degeneration (representing new muscle formation) was identified as smaller bundles of muscle fibers interspersed with collagen or fat. Total collagen was scored for the control group and groups 5, 6, 7, and 8. Refer to **Table 3** showing scoring designations for these trichrome

Table 2. Scoring Scale for Slides Stained with Immunohistochemistry

Score	Intensity of Stain
0	Negative
1	Weak staining in few areas
2	Weak staining in many areas
3	Moderate staining in many areas
4	Strong staining in many areas

Table 3. Scoring Scale for Slides Stained with Masson's Trichrome

Score	Collagen Organization[a]	Collagen Amount	Myocyte Degeneration[b]
0	Disorganized	None	None
1	Mildly Organized	Mild	Mild
2	Moderately Organized	Moderate	Moderate
3	Well Organized	Abundant	Abundant

[a] Parallel wavy collagen fibers with consistent blue color was considered to be more organized than collagen fibers that had variation of color and breaks in parallel fibers or infiltration.

[b] Distant fasciculi (myofibril bundles) or muscle with collagen infiltration was considered to have more myocyte degeneration than compact fasciculi without collagen infiltration.

stained slides. Statistical analysis was performed to determine significance with one-way ANOVA. Statistical significance was indicated by $p < 0.05$. Data determined to be statistically significant were further analyzed by pairwise multiple comparisons using Dunn's method ($p < 0.05$). Correlations were determined between collagen amount and collagen organization, collagen amount and myocyte degeneration, and collagen organization and myocyte degeneration by Microsoft Office Excel.

Results

Immunohistochemistry (IHC) of Paraffin-Embedded Tissues

In previous work from this laboratory, Masson's Trichrome staining was used to detect an increase of total collagen in the healed fascia of rats treated with CollaTape and fresh mesenchymal stromal cells (MSCs). These tissues also exhibited greater tensile strength than naturally healed rat fascia (Heffner *et al*., 2012). The current study aimed to determine if collagen type I (COLI) was the collagen fiber type responsible for these CollaTape repair observations.

Dilution Determination for Anti-Human Collagen Type I Primary Antibody:

In developing these methods, we first needed to determine the optimal dilutions to be used for the primary (binds to COLI) and secondary (biotinylated and binds to the primary) antibodies. Detection of COLI was first attempted with the α-human collagen I antibody diluted by a factor of 100 or 1000 with PBS (Thermo Scientific, Rockford, IL). The secondary antibody, α-Rabbit IgG, was diluted by a factor of 50 or 1000 in PBS (Invitrogen, Eugene, OR) (**Table 4**). Positive control slides were created for comparison using α-Rat IgG as the primary antibody at a dilution of 1:1000 (Vector Laboratories, Burlingame, CA) and the secondary antibody at a dilution of either 1:50 or 1:1000 in PBS. Results using this antibody indicated the presence of collagen but were indistinct due to high background tissue color change at low concentrations (**Table 4**). A dilution of 1:50 of the secondary antibody worked best with the positive control α- Rat IgG antibody. Increased background staining was observed on sections that were incubated

Table 4. Determination of Primary and Secondary Antibodies Dilutions[ab]

Primary Antibody (incubation for 60 minutes)	Primary Antibody Dilution Factor	Secondary Antibody Dilution Factor	Results/Staining Intensity (0-4)
α-Collagen I[c]	100	50	1
α-Collagen I	1000	50	2
α-Collagen I	100	1000	2[e]
α-Collagen I	1000	1000	2[e]
α-Rat IgG[d]	1000	50	3
α-Rat IgG	1000	1000	3

[a] All sections used in this experiment were from rat abdominal wall.

[b] Sections were stained using our standard paraffin IHC method. Antigen retrieval was not recommended with the primary antibody used on these sections. The quenching solution used was 2.7% H_2O_2 diluted in PBS for 20 minutes. The secondary antibody used on all slides was biotinylated goat anti-rabbit IgG antibodies. DAB was the chromogen used.

[c] Anti-Collagen I Polyclonal Antibody

[d] Biotinylated Anti-Rat IgG (H+L)

[e] May have been scored as 3 with the exception that darker areas suspected to be non-specific staining.

with the more diluted (1:1000) secondary antibody. At this time we had no explanation for why the lower antibody concentration resulted in higher background staining. It is possible that the timing of the 3, 3'-diaminobenzidine tetrahydrochloride (DAB) administration differed. The dilution of α-human collagen I primary antibody that yielded the best detection of COLI was 1:1000 with the secondary antibody diluted by a factor of 50. However, staining was only observed around the edges of the tissue and not at the wound site (**Figure 2**). Because of this unexpected result, background staining was still of concern and alterations were made to our standard IHC method to reduce background reactivity.

Addition of Rat Serum to Antibody Dilutions:

The first of these alterations was testing the incorporation of rat serum in the primary antibody diluents (Klinge *et al*., 2001). **Figure 3** shows how rat immunoglobulin in serum can bind non-specifically to Fc receptors of rat tissue and potentially block primary antibodies from binding to these non-specific sites. In this test, the primary antibody used on 4 slides was α-Rat IgG diluted by a factor of 1000 while 4 other slides were incubated with antibody diluents alone. Our standard IHC method was adhered to including quenching of endogenous peroxidase with 2.7% H_2O_2 for 20 minutes (see also **Table 6**). Sections, 2 each, were incubated with 150 µl of either PBS, rat serum, α-Rat IgG diluted in PBS or α-Rat IgG diluted in rat serum for one hour. The secondary antibody diluted in PBS by a factor of 50 was incubated with half of the sections that were incubated with each type of primary incubation reagent. The other half of sections was incubated with the secondary antibody diluted in PBS by a factor of 500.

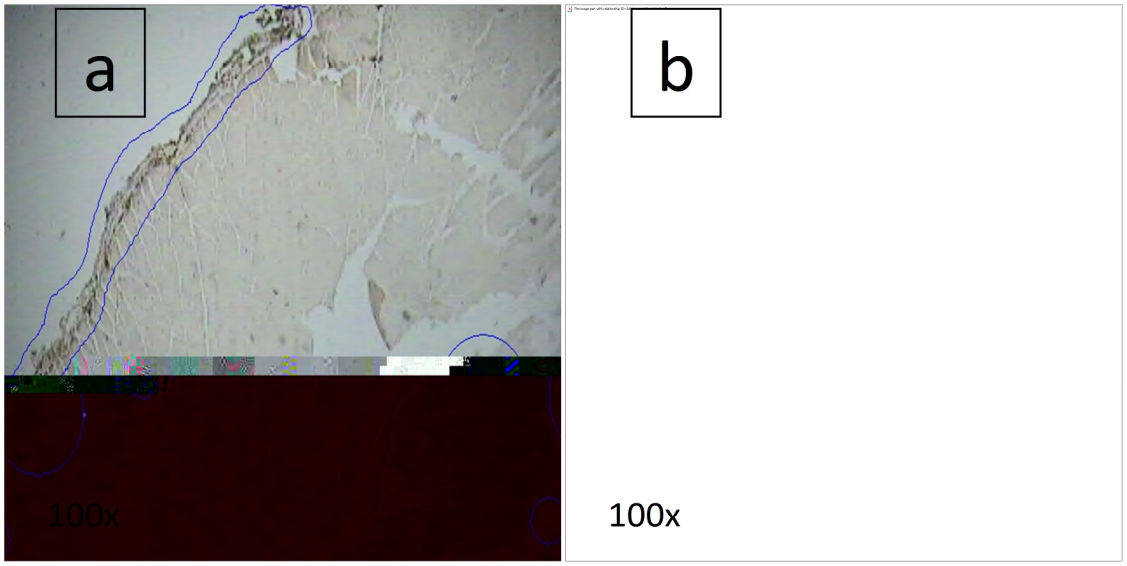

Figure 2. COLI Detection with Polyclonal Anti-Collagen I Antibody: The (a) edge and (b) wound site of a tissue section of abdominal wall from a rat of group 3a stained using our standard paraffin IHC method. This IHC method included quenching of endogenous peroxidase with 2.7% H_2O_2 for 20 minutes. The primary antibody used was rabbit α-human collagen I antibody diluted 1:100 with PBS. The secondary antibody used was biotinylated goat anti-rabbit IgG diluted 1:50 with PBS. The label used was 0.1 μg/ml streptavidin-horseradish peroxidase conjugate diluted with PBS. Sections were incubated with DAB chromogen substrate and a yellow/brown color change within the tissue indicated positive detection of COLI. Antigen retrieval was not performed. The tissue was photographed at 100x total magnification using MoticImage Plus 2.0. Both the (a) edges of a tissue section and the (b) wound site of the tissue section were photographed. Encircled blue areas indicate positive staining for COLI as indicated by a yellow/brown color due to a DAB colorimetric reaction.

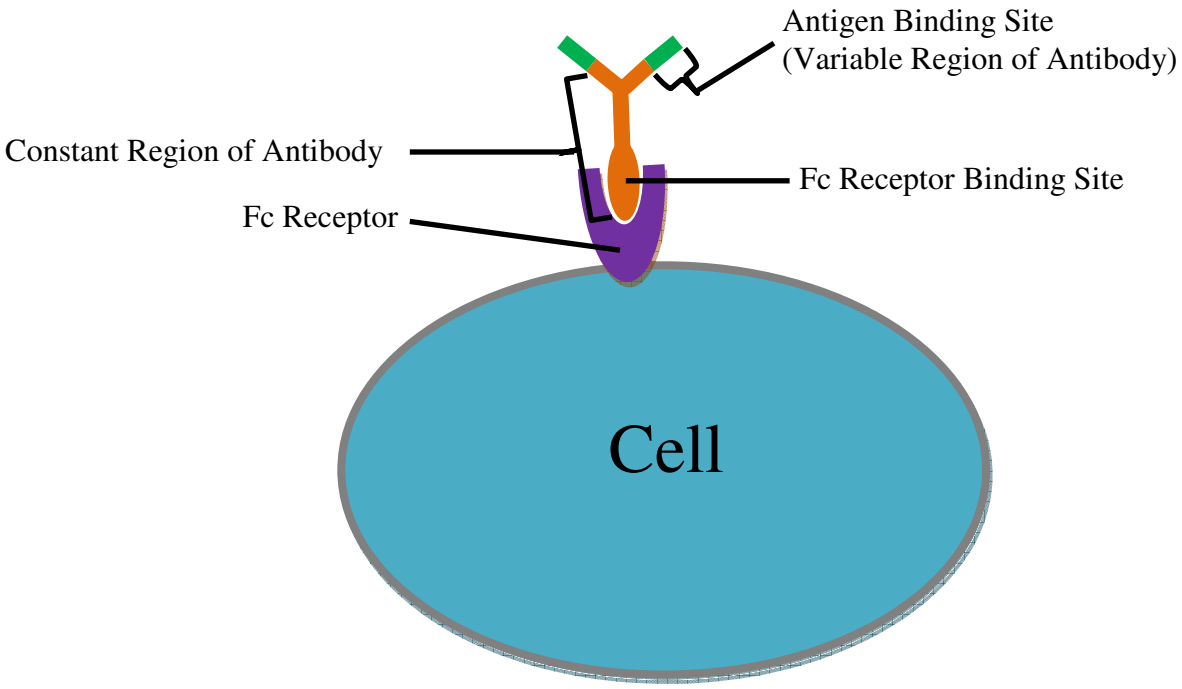

Figure 3. Antibody and Fc Receptor Binding Diagram: Antibodies non-specifically bind to Fc receptors on the surface of a cell.

Table 5 outlines this procedure and lists the resultant staining scores. Incubating sections with rat serum in place of the primary antibody incubation or as a primary antibody diluent increased the intensity and amount of staining indicating the antigen of interest. The rat serum increased the background staining, as well.

Quenching of Endogenous Peroxidases:

It was possible that our non-specific staining was due to endogenous peroxidases. Peroxidases are active within a number of cells and tissues including red and white blood cells and muscle. Peroxidase is also the enzyme that reacts with the DAB colorimetric substrate to produce a color change in tissues during IHC staining. In this study, peroxidase was conjugated to the streptavidin label and therefore would be indirectly bound to our target antigen when DAB was incubated with the sections. If endogenous peroxidases were not blocked, DAB is capable of reacting with these peroxidases causing non-specific staining. Hydrogen peroxide is commonly used as a peroxidase inactivating agent, and was used in this study. Refer to **Table 6** for the results obtained from testing a variety of quenching solutions on mouse spleen and reproductive organs and rat abdominal wall tissues. To test the blocking ability of the hydrogen peroxide, these tissues were not incubated with a primary or secondary antibody or streptavidin-horseradish peroxidase. DAB was incubated with sections directly following their incubation with the hydrogen peroxide. Rat abdominal tissues that were incubated with PBS instead of a hydrogen peroxide solution stained weakly in few areas or moderately dark in many areas (1 or 3) when the incubation lasted 15 or 20 minutes. Color change at

Table 5. Rat Serum as a Blocking Agent[ab]

Primary Antibody (incubation for 60 minutes)	Primary Antibody Dilution Factor	Secondary Antibody Dilution Factor (incubation for 20 minutes)	Results/Staining Intensity (0-4)
1X PBS	--	50	2
		500	3
Rat Serum	--	50	3
		500	3
α-Rat IgG	1000 in PBS	50	2
		500	3
α-Rat IgG	1000 in rat sera	50	4
		500	4

[a] All sections used in this experiment were from rat abdominal wall.

[b] Sections were stained using our standard paraffin IHC method. Antigen retrieval was not recommended with the primary antibody used on these sections. The quenching solution used was 2.7% H_2O_2 diluted in PBS for 20 minutes. The secondary antibody used on all slides was biotinylated goat anti-rabbit IgG antibodies. DAB was the chromogen used.

Table 6. Testing of Hydrogen Peroxide Quenching of Endogenous Peroxidases

Tissue Type	H_2O_2 Quenching Solution	Antibody Incubation[a]	Results/Staining Intensity[b] (0-4)
Male Rat Abdominal Wall Tissue	PBS for 15 minutes	None	3[b] (n=2)
Male Rat Abdominal Wall Tissue	PBS for 20 minutes	None	1, 3
Male Rat Abdominal Wall Tissue	0.03% H_2O_2 for 15 minutes	None	2[b]
Male Rat Abdominal Wall Tissue	0.3% H_2O_2 for 20 minutes	None	2
Male Rat Abdominal Wall Tissue	2.7% H_2O_2 for 15 minutes	None	3
Male Rat Abdominal Wall Tissue	2.7% H_2O_2 for 20 minutes	None	3
Male Mouse Spleen	PBS for 15 minutes	None	0[c], 1
Male Mouse Spleen	PBS for 20 minutes	None	1, 2[d]
Male Mouse Spleen	0.03% H_2O_2 for 15 minutes	None	0[c]
Male Mouse Spleen	0.3% H_2O_2 for 20 minutes	None	0
Male Mouse Spleen	2.7% H_2O_2 for 15 minutes	None	0
Male Mouse Spleen	2.7% H_2O_2 for 20 minutes	None	0
Female Mouse Reproductive Organs	PBS for 15 minutes	None	0[c]
Female Mouse Reproductive Organs	0.03% H_2O_2 for 15 minutes	None	0[c]
Female Mouse Reproductive Organs	0.3% H_2O_2 for 20 minutes	None	0
Female Mouse Reproductive Organs	2.7% H_2O_2 for 15 minutes	None	0

[a] Sections were not incubated with a primary or secondary antibody or the label, streptavidin-horseradish peroxidase. DAB was the chromogen substrate used on slides.

[b] Multiple areas within collagenous areas with high saturation of yellow/brown staining (not blood vessels).

[c] No yellow/brown staining but whole tissue turned dark.

[d] Large streak of yellow/brown staining running down half of the tissue sample (possibly outline of a blood vessel).

a score of 2 was observed within collagenous areas of the rat abdominal test sections when incubated with 0.03% H_2O_2 for 15 minutes (Caldwell *et al*., 2005). In an attempt to completely eliminate color reaction of DAB with endogenous peroxidase activity, more concentrated H_2O_2 solutions were tested (**Table 6**). The more concentrated H_2O_2 solution (2.7%) yielded staining similar to the PBS incubated rat abdominal tissues with a score of 3 while the 0.3% H_2O_2 solution reduced staining to a score of 2.

The mouse spleen tissues were tested as possible control tissues. These were also incubated with PBS for 15 or 20 minutes as well as the increasing concentrations of H_2O_2. DAB stained duplicate spleen tissues with an intensity of 0 or 1 when incubated with PBS for 15 minutes instead of H_2O_2. Spleen tissues were also incubated with PBS for 20 minutes yielding a staining score of 1 or 2. Mouse spleen and reproductive organ sections were incubated with increasing concentrations of H_2O_2 without primary or secondary antibody or streptavidin-horseradish peroxidase and did not yield areas of distinctive color change. Staining was scored at zero for the control slide for the mouse reproductive organs which was incubated with PBS for 15 minutes prior to DAB application. The female mouse reproductive organs were from older slides resulting in problems with the tissues washing off the slides. It was noted that the spleen tissues turned dark in a uniform fashion even though a score of 0 was given for DAB staining, as the staining did not appear to be specific when incubated with any concentration of H_2O_2 solution. For these reasons rat abdominal wall sections were the only tissue stained continuing through this study.

Background reactivity with H_2O_2 incubations did not yield successful results and it was suspected the background could be from another source. The conditions tested in

Table 6 were not successful in reducing non-specific staining in rat abdominal tissues and therefore we investigated more aggressive quenching methods (**Table 7**). The quenching solutions included 3% H_2O_2 that was heated to 70°C by microwave (Miller, 2001), 0.3% H_2O_2 diluted in PBS plus 0.1% sodium azide (NaAz) (Li *et al*., 1987), 2.7% H_2O_2 diluted in PBS and 0.3% H_2O_2 diluted in PBS. One section was incubated with each type of quenching solution after deparaffinization and hydration of the tissues by our standard IHC method. The heated H_2O_2 was incubated with the tissue section for 1 minute, the H_2O_2 and NaAz solution was incubated with its sections for 10 minutes, and the PBS diluted H_2O_2 solutions were incubated with their sections for 20 minutes. Sections were not incubated with a primary or secondary antibody or streptavidin-peroxidase. Slides treated with the heated 3% H_2O_2 and H_2O_2 with NaAz were incubated with DAB chromogen. The slides incubated with the varying concentrations of H_2O_2 for 20 minutes were not incubated with DAB chromogen. Sections incubated with heated 3% H_2O_2 at 70°C or 0.3% H_2O_2 with NaAz did not yield less background staining.

Staining with AEC Chromogen:

Because the background yellow/brown color was not being eliminated and was even present without DAB addition to slides (**Figure 4**), the colorimetric substrate aminoethyl carbazole (AEC) was tested instead of DAB to distinguish between areas of tissue that were detected by antibody binding to the antigen of interest and background reactivity. AEC stains the tissue red when it reacts with peroxidase and therefore would contrast with the yellow/brown debris (Tyrone *et al*., 2000).

Table 7. Additional Quenching Methods[ab]

H_2O_2 Quenching Solution[c]	DAB Chromogen Incubation (mins)	Results/Staining Intensity (0-4)
3% H_2O_2 at 70°C for 1 min[d]	10	3[e]
0.3% H_2O_2 with 0.1% NaAz for 10 mins	10	3[e]
0.3% H_2O_2 for 20 mins	0[g]	1[f]
2.7% H_2O_2 for 20 mins	0[g]	1[fg]

[a] All sections used in this experiment were from rat abdominal wall.

[b] Sections were not incubated with a primary or secondary antibody or the label, streptavidin-horseradish peroxidase. Sections were blocked per standard method. DAB was the chromogen substrate used on designated slides.

[c] Quenching solutions diluted to working dilutions using 1X PBS.

[d] Slide was not incubated in humidified chamber.

[e] Multiple areas within suspected collagen-rich areas with high saturation of yellow/brown staining (not blood vessels).

[f] A few areas of positive staining (yellow/brown) and many dark spots

[g] Most color change observed around tissue edges.

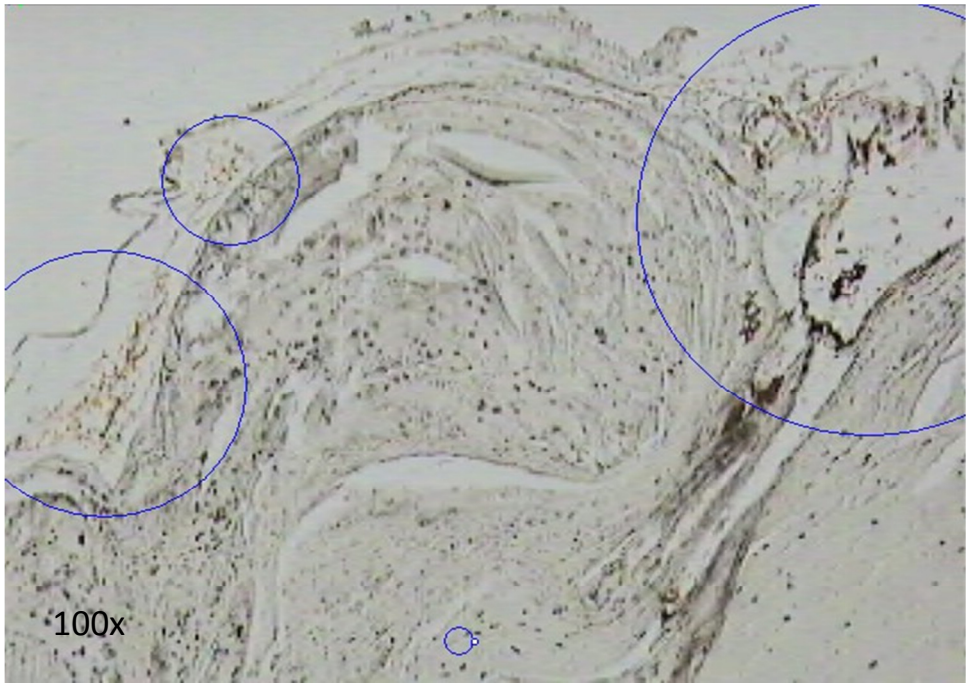

Figure 4. Background Staining in Negative Control: Image of background reactivity present in a negative control slide that did not include chromogen incubation. Our standard IHC method was performed on sections with the exception that sections were not incubated with a primary antibody, secondary antibody, HRP conjugate or chromogen. The slides were photographed at the wound site**.** The slide used for this image was incubated with a 0.3% H_2O_2 solution diluted in PBS for 20 minutes. Encircled blue areas indicate false positive yellow/brown staining.

A series of new ways to prepare negative control slides were first tested with the AEC chromogen (**Table 8**). Sections were deparaffinized and hydrated by our standard IHC method and incubated with 0.3% H_2O_2 for 20 minutes. One section was prepared as our previous negative controls were by replacing the primary antibody with only PBS during this 1 hour incubation and then continuing with the standard IHC method. Another section was incubated with PBS during the primary antibody and 20 minute secondary antibody incubation to test for any non-specific binding of the secondary antibody. Our standard IHC method was carried out as normal on the section after the secondary antibody incubation step while the third section was also incubated with PBS instead of streptavidin-horseradish peroxidase. After slides were developed with AEC, approximately 100 µl of ClearMount was applied to each slide and allowed to dry completely while baking on a 60°C heating block for 30 minutes. Slides were then dipped in xylene and mounted without dehydration through alcohol because AEC is alcohol soluble (Invitrogen, Frederick, MD). These experiments did not demonstrate non-specific staining resulting from the use of the AEC chromogen.

We next tested the ability to detect specific staining using α-Rat IgG or α-human collagen I as the primary antibody with AEC as the substrate (**Table 9**). The experimental slides were created with the primary antibody α-Rat IgG diluted with PBS by a factor of 100 and α-human collagen I was diluted with PBS by a factor of 1000. Each primary antibody was incubated with one section for one hour. All slides were incubated with the secondary antibody diluted by a factor of 50 and the standard IHC method was performed as normal with the exception of the AEC substrate substitution.

Table 8. New Preparation for Negative Controls Comparison[ab]

Secondary Antibody (incubation for 20 minutes)	Secondary Antibody Dilution Factor	Streptavidin-Horseradish Peroxidase Incubation (µg/ml)	Results/Staining Intensity (0-4)
α-Rabbit IgG[c]	50	0.1	0
PBS	--	0.1	0
PBS	--	0[d]	0

[a] All sections used in this experiment were from rat abdominal wall.

[b] Sections were stained using our standard paraffin IHC method. Antigen retrieval was not recommended with the primary antibody used on these sections. The quenching solution used was 0.3% H_2O_2 diluted in PBS for 20 minutes. Sections were not incubated with a primary antibody. AEC was the chromogen used.

[c] Biotinylated Goat Anti-Rabbit IgG Antibodies.

[d] PBS was incubated with section in place of streptavidin-HRP incubation.

Table 9. AEC Ability to Stain Sections[ab]

Primary Antibody[c] (incubation for 60 minutes)	Primary Antibody Dilution Factor	Results/Staining Intensity (0-4)
PBS	--	0[e]
α-Rat IgG[c]	100	0[e]
α-Collagen I[d]	1000	0[e]

[a] All sections used in this experiment were from rat abdominal wall.

[b] Sections were stained using our standard paraffin IHC method. Antigen retrieval was not recommended with the primary antibody used on these sections. The quenching solution used was 0.3% H_2O_2 diluted in PBS for 20 minutes. All sections were incubated with goat α-rabbit IgG secondary antibody diluted by a factor of 50. AEC was the chromogen used.

[c] Biotinylated Anti-Rat IgG (H+L)

[d] Anti-Collagen I Polyclonal Antibody

[d] Background staining along the entire section.

As **Table 9** shows, staining using the α-Rat IgG or α-human collagen I was very weak and indicated the need for a new primary antibody.

Use of Antigen Retrieval with Anti-Rat Collagen Type I Primary Antibody:

The primary antibody was changed to α-Rat COLI. Antigen retrieval with a heated citrate buffer method was recommended for optimal antigen detection with this antibody. Antigen retrieval was performed with a variety of methods (AbCam, 2010). Sections were first deparaffinized and hydrated as in our standard IHC method. Sections were incubated with 0.3% H_2O_2 for 20 minutes. Antigen retrieval was performed by immersing slides into 95°C sodium citrate buffer (0.01M) for 2 minutes and then 30 second heating intervals for duration of 5 minutes. A microwave was used to control the temperature of the sodium citrate buffer. A total of 2 sections were incubated with the α-Rat COLI primary antibody diluted by a factor of 100 or 1000 on respective sections (**Table 10**). Our standard IHC method was adhered to for the rest of the procedure with the exception of AEC colorimetric substrate substitution. **Table 10** and **Figure 5** show the results for slides stained to detect COLI when subjected to the microwave antigen retrieval method. These slides were absent of color similar to its negative controls or stained very lightly. These slides were stained with α-Rat COLI and background debris was abundant at any dilution.

This same procedure was repeated with the α-Rat COLI antibody diluted by a factor of 1000 but with different antigen retrieval methods. The additional antigen

Table 10. Antigen Retrieval by Microwave Method[ab]

Primary Antibody (incubation for 60 minutes)	Primary Antibody Dilution Factor	Secondary Antibody (incubation for 20 minutes)	Secondary Antibody Dilution Factor	Streptavidin-Horseradish Peroxidase Incubation (µg/ml)	Results/Staining Intensity (0-4)
α-Rat COLI[g]	1000	α-Rabbit IgG[h]	50	0.1	1[df]
α-Rat COLI	100	α-Rabbit IgG	50	0.1	0[de]
PBS	--	α-Rabbit IgG	50	0.1	0[de]
PBS	--	PBS	--	0[c]	0[de]

[a] All sections stained were rat abdominal tissues.

[b] Antigen retrieval was performed by immersing slides into 95°C sodium citrate buffer (0.01M) for 2 minutes and then 30 second heating intervals for duration of 5 minutes. A microwave was used to control the temperature of the sodium citrate buffer. The quenching solution used was 0.3% H_2O_2 diluted in PBS for 20 minutes. AEC was used as the chromogen substrate for these sections.

[c] PBS was incubated with the section in place of streptavidin-HRP incubation.

[d] Yellow/brown grainy background reactivity present.

[e] Some areas hard to observe due to poor mounting.

[f] Few collagenous areas stained positive.

[g] Anti-Rat Collagen Type I

[h] Biotinylated Goat Anti-Rabbit IgG Antibody

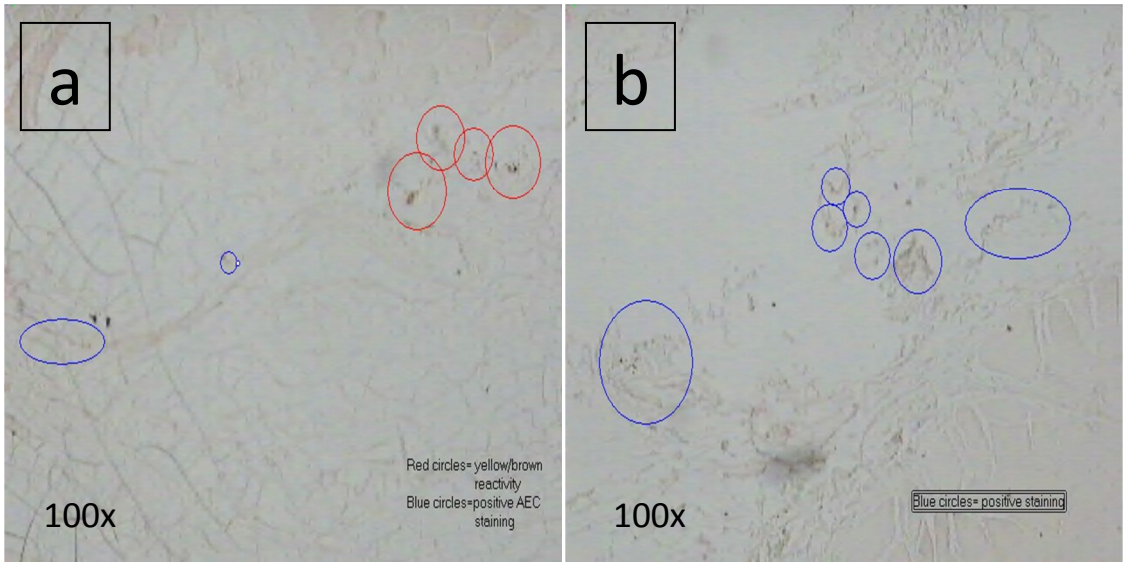

Figure 5. Determining the Dilution for the Primary Antibody: Detection of COLI at the wound site of sections using anti-rat collagen type I primary antibody at dilutions of (a) 1:100 and (b) 1:1000. The sections were stained using our standard paraffin IHC method. The quenching solution was 0.3% H_2O_2 diluted with PBS for 20 minutes. With the use of a microwave, a heated sodium citrate antigen retrieval method was used on these sections. Slides were incubated with the primary antibody α-Rat COLI at either (a) 1:100 or (b) 1:1000 diluted with PBS. The secondary antibody and HRP conjugate label were applied as described in **Figure 2**. Sections were incubated with AEC chromogen substrate and a red color change within the tissue indicated positive detection of COLI. Encircled red areas indicate background staining as indicated by a yellow/brown color. Encircled blue areas indicate positive staining for COLI as indicated by a red color resulting from an AEC colorimetric reaction.

retrieval methods tested used a water bath to heat the sodium citrate buffer and a 2 hour bake of slides with allowance to cool prior to staining. Sections were immersed in the buffer at 75°C for 10 or 30 minutes or 95°C sodium citrate buffer for 20 minutes. When slides were immersed in heated citrate buffer (using a water bath) for 30 minutes tissues washed off the slides following the antigen retrieval method. Antigen retrieval by water bath heated citrate buffer for 10 minutes yielded more intense color change of tissues on experimental slides but this color change was also observed on the negative controls in this experiment (**Table 11**). Slides in a 95°C citrate buffer bath for 20 minutes yielded light detection of COLI at a score of 1 on the experimental slide and no color change on its negative control (**Table 12**). **Figure 6** shows an area detecting COLI from a slide prepared with this antigen retrieval method (95°C for 20 minutes). Staining with the new antibody appeared to be specific but weak.

Intensification of Staining with DAB Enhancers:

To improve the intensity of staining, DAB enhancement techniques were tested next (Werner *et al*., 1996) (**Table 13**). These enhancement techniques require the use of DAB rather than AEC as the chromogen. However, they also affect the color of the stained sections and we hoped that this would allow us to differentiate specific staining from background debris. Our standard IHC method was performed on 8 sections which were incubated with 0.3% H_2O_2 for 20 minutes. Antigen retrieval was performed by immersing the slides in 95°C sodium citrate buffer (water bath heated) for 20 minutes. The primary antibody used was α-Rat COLI (1:1000 in PBS). DAB was mixed

Table 11. Heat Induced (75°C) Antigen Retrieval[ab]

Primary Antibody (incubation for 60 minutes)	Primary Antibody Dilution Factor	Results/Staining Intensity (0-4)
α-Rat COLI[c]	1000	1 [e]
α-Rat Myosin[d]	80	1 [e]
PBS	--	1[e]

[a] Refer to **Table 10** for source of sections stained.

[b] Sections were baked for 2 hours and allowed to cool to room temperature prior to IHC staining. The standard paraffin IHC method was adhered to. Antigen retrieval was performed by immersing slides into 75°C sodium citrate buffer (0.01M) for 10 minute duration. A water bath was used to control the temperature of the sodium citrate buffer. The quenching solution used was 0.3% H_2O_2 diluted in PBS for 20 minutes. All sections were incubated with biotinylated goat α-rabbit IgG secondary antibody diluted by a factor of 50. AEC was used as the chromogen substrate for these sections.

[c] Anti-Rat Collagen Type I

[d] SC-71 Hybridoma Anti-Rat Myosin Heavy Chain

[e] Mounting media bubble formed in procedure and not able to coverslip therefore not much of tissue easily seen.

Table 12. Heat Induced (95°C) Antigen Retrieval[ab]

Primary Antibody (incubation for 60 minutes)	Primary Antibody Dilution Factor	Results/Staining Intensity (0-4)
α-Rat COLI[c]	1000	1[d]
PBS	--	0[de]

[a] Refer to **Table 10** for source sections stained.

[b] Sections were baked for 2 hours and allowed to cool to room temperature prior to IHC staining. The standard paraffin IHC method was adhered to. Antigen retrieval was performed by immersing slides into 95°C sodium citrate buffer (0.01M) for 20 minutes. A water bath was used to control the temperature of the sodium citrate buffer. The quenching solution used was 0.3% H_2O_2 diluted in PBS for 20 minutes. All sections were incubated with biotinylated goat α-rabbit IgG secondary antibody diluted by a factor of 50. AEC was used as the chromogen substrate for these sections.

[c] Anti-Rat Collagen Type I

[d] Yellow/brown grainy background reactivity (moderate amount) present.

[e] One collagenous area contained approximately 5 darker pink spots (nuclear-like shape) in a concentrated area.

Figure 6. Testing of a Sodium Citrate Antigen Retrieval Technique: Sections were baked for 2 hours and allowed to cool to room temperature prior to IHC staining. The standard paraffin IHC method was adhered to. Sections were incubated with 0.3% H_2O_2 solution diluted in PBS for 20 minutes. Antigen retrieval was performed by incubating sections in a sodium citrate buffer (pH 6.0) in a 95°C water bath for 20 minutes. The primary antibody, α-Rat COLI, was diluted by a factor of 1000 with PBS. Sections were incubated with the same secondary antibody and HRP conjugate label as described in **Figure 2**. Sections were incubated with AEC chromogen substrate. Encircled blue areas indicate positive staining for COLI as indicated by a red color resulting from an AEC colorimetric reaction.

Table 13. Testing Addition of DAB Enhancers[ab]

Primary Antibody (incubation for 60 minutes)	Primary Antibody Dilution Factor	DAB Enhancer[c]	Results/Staining Intensity (0-4)
α-Rat COLI[d]	1000	0.0013M CoCl	2[e]
PBS	--	0.0013M CoCl	2[e]
α-Rat COLI	1000	0.01M Imidazole	1[fg]
PBS	--	0.01M Imidazole	1[g]
α-Rat COLI	1000	DAB Kit Enhancer	0[h]
PBS	--	DAB Kit Enhancer	0[h]
α-Rat COLI	1000	0.05% $NiCl_2$	0[i]
PBS	--	0.05% $NiCl_2$	0[g]

[a] Refer to **Table 10** for source of sections stained.

[b] Refer to **Table 12** for IHC method with alterations used for these sections.

[c] DAB was used as the chromogen substrate for these sections. Various solutions were added to the DAB to enhance the staining capabilities.

[d] Anti-Rat Collagen Type I

[e] Collagenous areas stained but difficult to tell if specific areas detected for COLI since everything stained rather dark.

[f] RBCs, WBCs and blood vessels stained very well and some nuclei stained well.

[g] Little or no prior yellow/brown grainy background staining noticed.

[h] A lot of (black) precipitate everywhere

[i] Prior background present.

according to manufacturer's instructions and had 50 µl of the kit's enhancer, 0.0013M cobalt chloride, 0.01M imidazole, or 0.05% nickel chloride added to it. Each DAB mixture was incubated with 1 experimental slide (to detect COLI) and 1 negative control slide. **Table 13** shows the results from incubating slides with the enhanced DAB solutions. Adding cobalt chloride or imidazole to the DAB colorimetric substrate decreased background reactivity in the tissues but staining could not be classified as specific. There was no background debris observed on slides that were incubated with the DAB and imidazole colorimetric solution but vasculature and blood cells stained brightly. None of the samples incubated with an enhanced DAB solution had significant staining when compared to their respective negative control slide. A summary of all the tested alterations of our standard IHC method along with the results for each test is shown in **Table 14**.

Table 14. Summary of Alterations to IHC Method[a]

Primary Antibody	Quenching (conc. and time)	Chromogen Substrate	Secondary Antibody[b] (1:50)	Citrate Antigen Retrieval	Results
None	0.03% for 15 mins	DAB	None	None	False Positive
	0.3% for 20 mins	None			
		AEC		95°C (microwave)	
	2.7% for 20 mins	None		None	
		DAB			
	0.3% for 20 mins	AEC		75°C for 30 mins	Tissue washed off
			+	75°C for 10 mins	Intentional negative
				95°C for 20 mins	
α-Collagen I[c]				None	Negative
α-Rat COLI[d]				95°C (microwave)	Weak Positive
			None	75°C for 30 mins	Tissue wash off
			+	75°C for 10 mins	Unintentional Negative
				95°C for 20 mins	Weak Positive

[a] Refer to **Table 4** for source of sections stained.

[b] Biotinylated Goat Anti-Rabbit IgG Antibody

[c] Anti-Collagen I Polyclonal Antibody at dilutions of 1:100 and 1:1000

[d] Anti-Rat Collagen Type I at dilution of 1:1000

+ = Slides incubated with secondary antibody at 1:50 dilution and streptavidin-horseradish peroxidase at 0.1 µg/ml.

Effect of AlloMax Mesh on Wound Healing

AlloMax is a common surgical graft used during hernia repair and preferred for its high resistance to tension attributed to its pure dermal collagen composition (Bard, 2010). **Figure 7** illustrates an example of abdominal wall taken from a control, uninjured rat stained with Masson's Trichrome stain. This slide shows high collagen organization and low to moderate collagen amount with no myocyte degeneration. The collagen is stained blue with Masson's Trichrome. The upper layer of collagen is the external fascia that overlies the abdominal wall. The collagen between the two muscle areas is the linea alba. Tissues sections in **Figures 8a**, **8b**, and **8d** are similar in collagen amount and organization to **Figure 7**. These figures show representative examples of tissue sections taken from experimental animals whose abdominal incisions were treated with AlloMax only (**Figure 8a**), AlloMax with PRP (**Figure 8b**), or AlloMax with PRP and fresh MSCs (**Figure 8d**), respectively. It is apparent from these pictures that the tissue repaired with AlloMax and fresh MSCs (**Figure 8c**) has more collagen than the control tissue (**Figure 7**).

Trichrome stained slides from AlloMax treated groups were scored by 2 blinded observers using the scale shown in **Table 3** to find a mean score of collagen organization and amount, and myocyte degeneration for each group. Means and standard deviations were calculated for a total of 5 groups, which included a control (uninjured) group, rats repaired with AlloMax only group, rats repaired with AlloMax and PRP group, rats repaired with AlloMax and fresh MSCs group, and rats repaired with AlloMax, PRP and fresh MSCs group. **Figures 9, 10** and **11** compares the features of the abdominal walls excised from rats of each group 8 weeks after surgery. **Figure 9** shows that tissue of rats

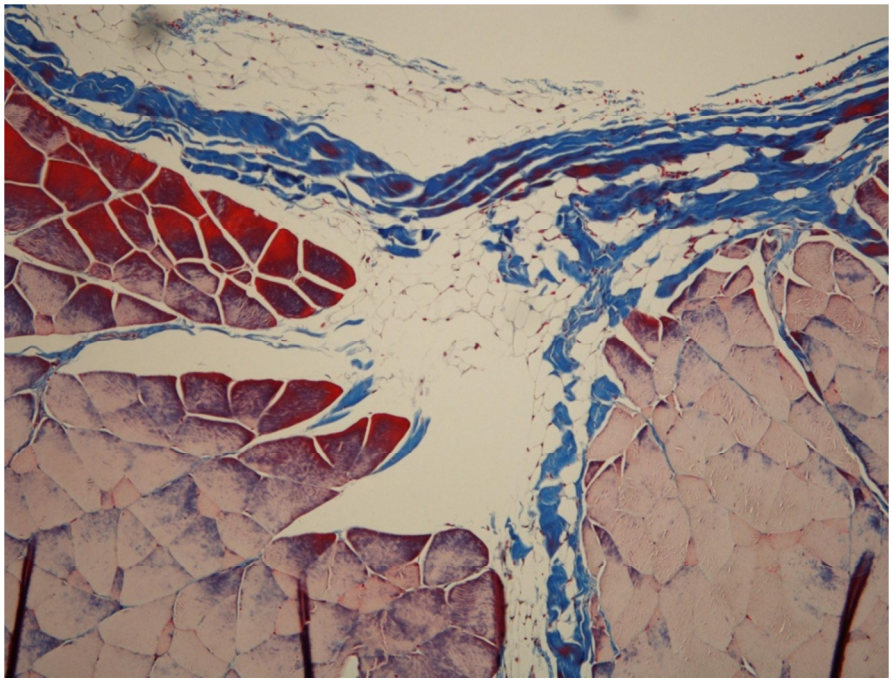

Figure 7. Control Slide Stained with Masson's Trichrome: Representative slide prepared from abdominal wall tissue of an uninjured, control rat.

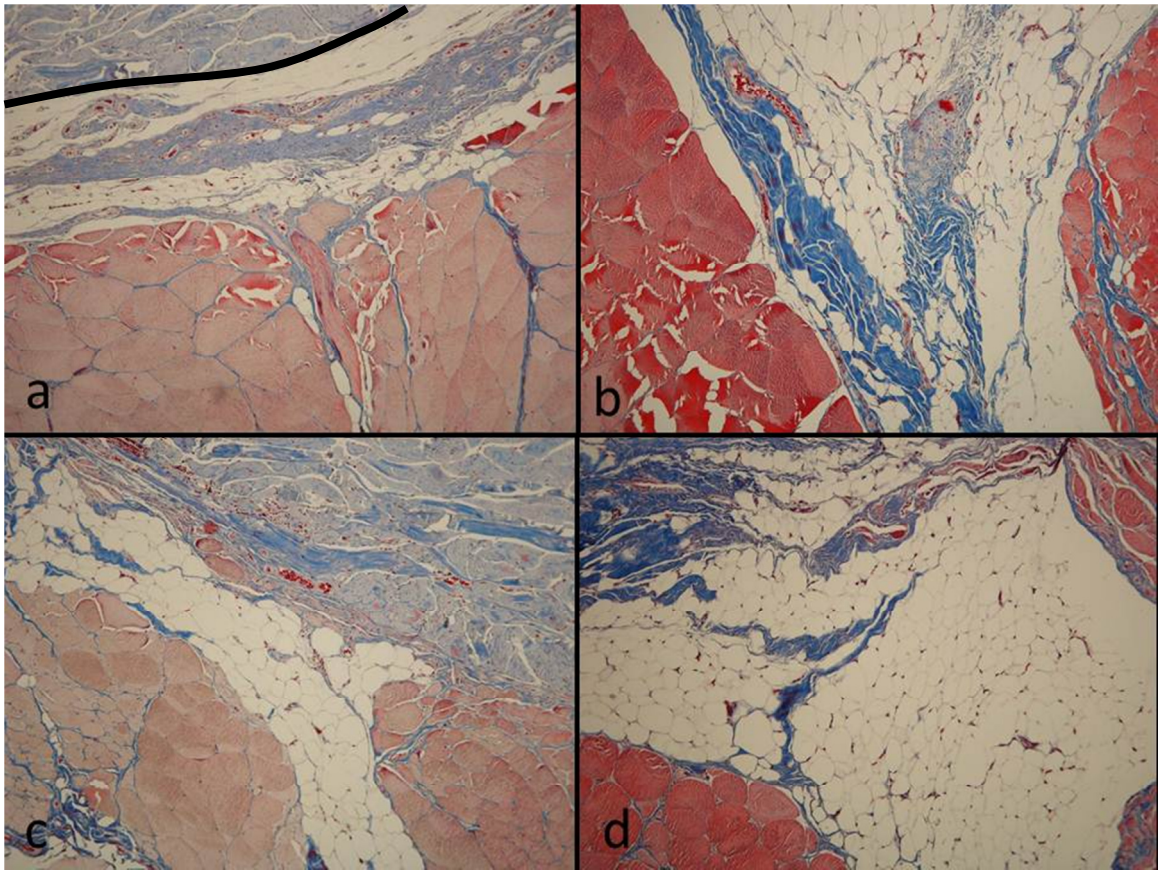

Figure 8. Experimental Slides Stained with Masson's Trichrome: Representative pictures of abdominal wall tissue of rats receiving (a) AlloMax only, (b) AlloMax and PRP, (c) AlloMax and MSCs and (d) AlloMax, PRP, and MSCs. Blue staining indicates collagen. Red staining indicates abdominal wall muscle. Area above black line of 8a is AlloMax mesh and was not included in scoring of this slide.

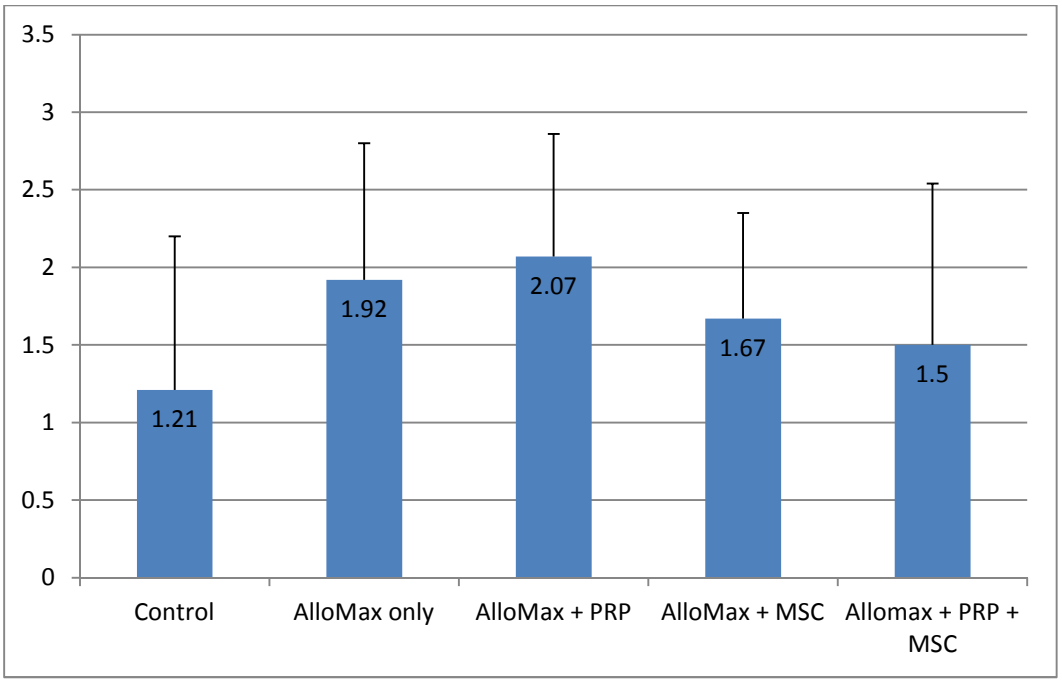

Figure 9. Comparison of Collagen Organization between Groups: Average scores obtained for each group from 2 blinded observers. Results shown for tissues collected 8 weeks post-operative. AlloMax + MSC and AlloMax only groups were each (n=6), all other groups (n=7). Data represents the mean (+/- SD). Statistical analysis was performed using a one-way ANOVA. No significant differences were seen between groups.

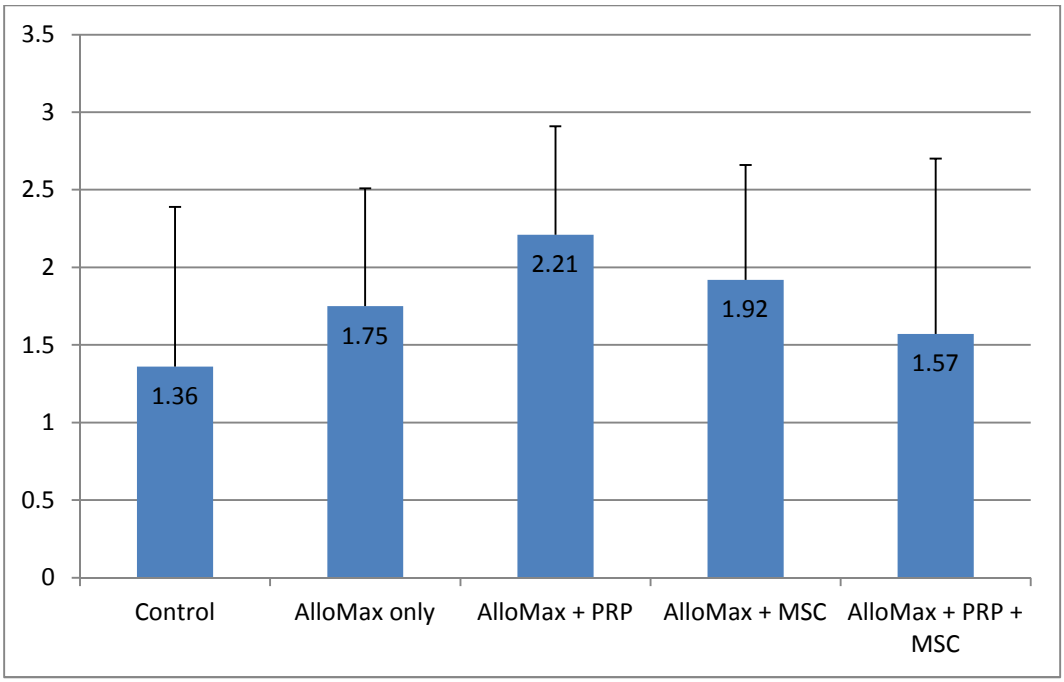

Figure 10. Comparison of Collagen Amount between Groups: Groups and blinded observers are the same as in **Figure 9**. Data represents the mean (+/- SD). Statistical analysis was performed using a one-way ANOVA. No significant difference was seen between groups.

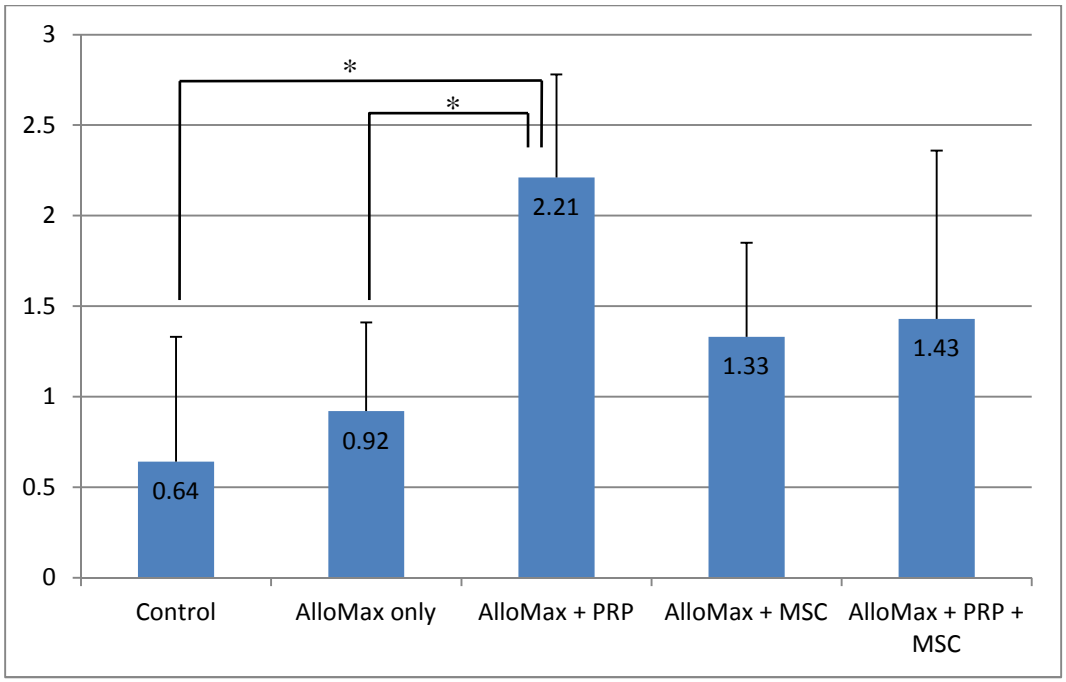

Figure 11. Comparison of Myocyte Degeneration between Groups: Groups and blinded observers are the same as in **Figure 9**. Data represents the mean (+/- SD). Statistical analysis was performed using a one-way ANOVA. Statistical significance was examined using pairwise multiple comparisons (Dunn's method) (* = $p < 0.05$).

that had AlloMax with PRP applied showed the most collagen organization with a mean score of 2.07 (± 0.79) of a possible score of 3 indicating moderately organized collagen followed by the AlloMax only group at 1.92 (± 0.88). Tissue from rats treated with AlloMax and fresh MSCs had an average score of 1.67 (± 0.68) for collagen organization. The group repaired with AlloMax, PRP and fresh MSCs had the least collagen organization among the experimental groups with a mean score of 1.50 (± 1.04). However, all experimental groups had higher mean scores for collagen organization than the control group (1.21 ± 0.99). Statistical significance was not found between groups.

The AlloMax with PRP group also had the highest average score for collagen amount at 2.21 (± 0.70) (**Figure 10**). Rats repaired with AlloMax and fresh MSCs had a mean score of 1.92 (± 0.74) followed by the Allomax only group (1.75 ± 0.76) and lastly the AlloMax, PRP and fresh MSC group at 1.57 (± 1.13) for collagen amount. The tissue of control rats had the least amount of collagen with an average score of 1.36 (± 1.03). Collagen amount was not found to be significantly different between groups.

Myocyte degeneration, seen as separation of myofibril bundles with collagen or fat, was scored for tissues of all the rat groups and the mean scores were found for the 8 week post-operative groups (**Figure 11**). The control group was found to have the least amount of myocyte degeneration with an average score of 0.64 (± 0.69). An average score of 0.92 (± 0.49) was calculated for abdominal wall that had only AlloMax applied to it. Myocyte degeneration gradually increased from the AlloMax with fresh MSC group (1.33 ± 0.52) to the AlloMax, PRP and fresh MSC group (1.43 ± 0.93). The greatest amount of myocyte degeneration (2.21 ± 0.57) was observed for tissue repaired with AlloMax with PRP. Myocyte degeneration was significantly increased in the

abdominal wall that was repaired with AlloMax and PRP and allowed to heal for 8 weeks, when compared to uninjured abdominal wall or repair with the AlloMax surgical mesh only ($p < 0.05$).

Correlations between the scores given to trichrome stained slides for myocyte degeneration, collagen organization and collagen amount were determined for each of the tested traits (**Table 15**). The slope and correlation value (R^2) was determined for each group. A positive correlation was found between collagen organization and amount among all groups but only the AlloMax + PRP + fresh MSC group ($R^2 = 0.941$) and the control group ($R^2 = 0.871$) had high correlations. Myocyte degeneration was not correlated to collagen organization or amount in control abdominal wall sections. However, scores from trichrome stained sections of rats repaired with AlloMax and PRP showed a negative correlation between the separate collagen traits and myocyte degeneration. Correlations of collagen organization with myocyte degeneration and collagen amount with myocyte degeneration were analyzed and significant correlations were not found.

Table 15. Correlations of Scored Abdominal Wall Characteristics

	Collagen Organization vs. Collagen Amount		Collagen Organization vs. Myocyte Degeneration		Collagen Amount vs. Myocyte Degeneration	
	Slope	*R^2 Value*	*Slope*	*R^2 Value*	*Slope*	*R^2 Value*
Control	0.965	0.871	0.168	0.038	0.362	0.188
AlloMax Only	0.672	0.699	0.086	0.015	0.280	0.100
AlloMax + PRP	0.648	0.590	-0.472	0.313	-0.573	0.328
AlloMax + MSC	1.00	0.748	0.350	0.175	0.262	0.131
AlloMax + PRP + MSC	1.04	0.941	0.222	0.050	0.296	0.101

Discussion

One of the functions of the abdominal wall is to serve as a barrier between the organs of the abdominal cavity and outside world. The fascia and muscle layers experience more pressure from the intestines and other organs in the abdominal cavity than does the skin of the abdominal wall. Abdominal wall integrity may greatly suffer following an abdominal surgery, especially the musculo-fascial layers. Scar tissue is always weaker than the uninjured tissue it replaces. Therefore, abdominal surgery puts patients at a high risk for hernia formation and subsequent recurrences (DuBay *et al*., 2007). Collagen is the primary structural element of fascia and substantially contributes to its strength or compliance (Junqueira *et al*., 1992). The process of wound healing has been examined in great detail but many studies have focused on the repair of skin. The current study is unique in that it aimed to discover the total and specific type of collagen content within the musculo-fascial layers of the abdominal wall of rats following an abdominal incision, with an examination of the effect mesenchymal stromal cell (MSC) supplementation may have on collagen redistribution with or without platelet-rich plasma (PRP) priming.

Previously, studies from our lab have shown that abdominal wounds healed with CollaTape, PRP and fresh MSCs have 117% increased tensile strength and significantly greater amounts of collagen, when compared to naturally healed abdominal incisions (Heffner *et al*., 2012). There is a suspected correlation between these 2 MSCs stimulated effects. Collagen type I (COLI) is made of strong, uniform fibers allowing it to resist tension (Junqueira *et al*., 1992). The present study was designed to detect COLI in these stronger, collagen abundant abdominal wall sections. A study by Madden and Peacock

(1971) reported that after 3 weeks of healing, scar tissue strength is attributable to either collagen organization or replacement by stronger collagen types. Because collagen organization was similar between all groups treated with CollaTape with or without MSCs (Heffner *et al*., 2012), it is highly probable that the majority of collagen within MSC treated wounds is COLI fibers.

Collagen fibers share basic structural similarities but the slight differences in each fiber type's molecular composition can be detected by antigens on the surface of these fibers. Immunoassays use antibodies that attach specifically to particular antigens. One type of immunoassay commonly used is enzyme-linked immunosorbent assays (ELISAs). In a study testing MSCs ability to synthesize collagen, an ELISA was used to successfully measure COLI of *in vitro* samples. Results of the ELISA showed that MSCs accelerate COLI production significantly by identifying these particular fibers in comparative samples (Han *et al*., 2005). Performing an ELISA is simple and provides quantitative results but requires the use of fresh tissue samples. In order to compare collagen organization and amount between rats in our previous study the abdominal tissues were paraffin-embedded, sectioned, and fixed onto slides (Heffner *et al*., 2012). Only 1 slide was stained with Masson's Trichrome for each rat and several other slides were stored for future studies. In the current study, the method in which collagen fiber types could be detected was limited to histological analysis because these extra slides were available for use but fresh tissue samples were not.

Many stains, such as Masson's Trichrome, identify a general group of molecules but are unable to differentiate between subtypes within that group. Immunohistochemistry (IHC) is a popular staining method that is based on the concept

that antibodies bind to their specific antigens. Antigens of interest within a tissue sample can be visualized using IHC, making it possible for tissue composition to be specifically analyzed. Both the location and semi-quantitative amounts of the selected antigen/molecular tissue component can be determined with IHC (Werner *et al*., 1996). Some other advantages of IHC include a relatively low cost and easy method. Much of the equipment needed for a standard IHC protocol can be found in even the most basic of laboratories and antibodies are usually the most costly supplies (Leong and Leong, 2011).

COLI was found in the fascia of human abdominal walls by using IHC staining techniques in a study comparing the collagen content of patients with or without hernias (Klinge *et al*., 2001). This study was able to definitively show that COLI is decreased in scar tissue associated with a hernia compared to healed abdominal incisions that did not result in a hernia. IHC staining was successful for this human study but this method could not be replicated in our samples because frozen tissue sections were used in the Klinge *et al* (2001) study. Performing IHC on paraffin-embedded sections can be widely different from the steps taken to stain frozen sections. As seen in this study, paraffin-embedded tissues do not always stain well. Staining paraffin-embedded tissues may be difficult with IHC because of incompatible fixation methods or the reduced availability of antibodies that work with these tissues. Background staining or other non-specific types of staining are common problems encountered with IHC staining of frozen or paraffin-embedded sections (Leong and Leong, 2011).

White *et al.* (2007) was able to use IHC on human paraffin-embedded fascia sections to specifically stain COLI. Their IHC method included an antigen retrieval step, incubation with 3% hydrogen peroxide (H_2O_2) and a 3, 3'-diaminobenzidine

tetrahydrochloride (DAB) chromogen. While the rat paraffin-embedded sections of this study were stained using similar IHC steps as described by White and collaborators, our staining was unsuccessful. Details were not published about the fixation procedure of these human tissues or the dilutions of the antibodies used on sections which therefore made it impossible to duplicate the procedure. Alternatively, rat tissue may be more sensitive to formaldehyde fixation than human tissue and thus may require unique practices to detect the antigens of interest.

The first few experiments of this study tested the antibody dilutions to be used. All of the antibodies used in this study were concentrated and therefore needed to be diluted before use. We tested dilutions within the manufacturer's recommended dilution range for each antibody (Thermo Scientific, Rockford, IL; Vector Laboratories, Burlingame, CA),. The data shown in **Table 5** provided better evidence for the working dilution of the secondary antibody than for the primary. The secondary antibody diluted by a factor of 50 did not produce the darkest staining, but the staining observed on these slides was concentrated to collagenous areas. Slides incubated with the secondary antibody at a dilution of 1:1000 (Invitrogen, Eugene, OR) had staining within the muscle and vascular structures, where COLI is less likely. Although sections stained better with a working dilution of 1:1000 for anti-human collagen I primary antibody, no staining was detected at the wound site for any samples. The staining that was scored for anti-human collagen I experiments (with either DAB or aminoethyl carbazole color detection) was isolated to the edges of tissue sections which raised doubt about its specificity and a new antibody was purchased to continue testing. After further evaluation this staining may have been true staining. This type of staining is classified as an "edge effect" and

happens when the edges of sections were fixed better than the middle or because the edges of the tissue lift up from the slide allowing antibodies to attach to the underside of tissues (Leong and Leong, 2011).

In an attempt to highlight the specifically stained areas of the tissue, rat serum was tested as a possible primary antibody diluent instead of phosphate-buffered saline (PBS). The rat serum had an adverse effect on staining specificity. Sections stained more intensely with the incorporation of rat serum but specifically stained areas were more difficult to distinguish. The rat serum was used to dilute α-Rat immunoglobulin G (IgG) used as a primary antibody. Rat serum contains rat IgG which could bind to the variable region of the primary antibody against rat IgG. This may have prevented the anti-rat IgG from binding to its intended target and allowing more areas of the tissue to develop background color change, resulting in a false positive.

Background color change is usually defined as coming from either endogenous peroxidase or biotin in tissue sections. If endogenous biotin is not blocked, the streptavidin-horseradish peroxidase label will not specifically bind to the biotinylated secondary antibody which is linked to the primary antibody, but will attach to other biotin molecules in the tissue causing false positive results (Atwood and Dako Technical Support Group, 2009). This was not an observed problem in our sections. Our study also tested quenching solutions to determine the amount of endogenous peroxidase activity in the rat tissues. This peroxidase activity can be irreversibly inactivated by reacting with large amounts of H_2O_2 which ensures that the subsequent colorimetric substrate only reacts with the peroxidase conjugated to the streptavidin, thus only detecting the antigen of interest (Kobayashi *et al*., 1987). H_2O_2 concentrations and incubation times were

varied without primary antibody incubation in an attempt to reduce endogenous peroxidase reacting with the DAB colorimetric substrate. Incubating sections with a stronger concentration of H_2O_2 did not yield better results. In fact, 2.7% H_2O_2 did not reduce background when compared to its control slide that was incubated with PBS instead of a quenching solution. Slides incubated with 2.7% H_2O_2 were stained darker than slides with 0.03% or 0.3% H_2O_2 without primary antibody incubation. Slides that were pre-treated with 0.3% H_2O_2 had the least amount of background staining but background was never completely eliminated. The background color observed after IHC staining was suspected to be from a source yet to be discovered, possibly an artifact introduced during processing of the tissues. The time of incubation for quenching was set to 20 minutes instead of shorter times of 1, 10 or 15 minutes for all slides after this set of experiments not because less peroxidase activity was detected but because deleterious effects were not observed at this longer incubation time.

Due to the consistently unremarkable results of experimental slides compared to their respective controls, it was feared that background staining was never really eliminated from the sections by the IHC method being performed. **Table 7** shows that even with extreme changes in the quenching solution (Miller, 2001; Li *et al*., 1987), tissues stained intensely following DAB incubation. The same table also illustrates that the DAB chromogen was not contributing to this intense staining alone. Tissues expressed a yellow/brown color change in the tissue with only H_2O_2 incubation. Slides were found to sometimes have these areas of yellow/brown discoloration around the tissue sections prior to beginning IHC. The yellow/brown color developed on a majority of slides during the fixation process.

The anti-rat COLI primary antibody that was purchased after questioning the specificity of the original anti-human collagen I primary antibody recommended performing antigen retrieval on sections for optimal detection of COLI (Millipore, Temecula, CA). Before antigen retrieval was developed, few paraffin-embedded sections could be stained with IHC. Tissues are fixed immediately following excision from a subject. During fixation, tissues are kept in a fixative reagent, usually formalin. Formaldehyde is the main component of formalin, which is responsible for forming cross-bridges between the end terminals of proteins in tissue samples during fixation. These cross-bridges may cover the epitopes of antigens within a tissue section and therefore make it incredibly difficult for the antibody to detect the antigen during an IHC procedure (Mortensen and Brown, 2011). Antigen retrieval provides a possible way to sever these unwanted bonds and expose the once hidden epitopes (True, 2008). Although antigen retrieval was determined to improve staining slightly, staining was never considered strongly positive.

If tissues are left in formalin for too long, permanent cross-bridges have been known to form. It is hard to identify what time period would be too long, since the fixation process for tissues varies widely between samples depending on size and origin. Thinner tissues, like that used in this study, however may only need to stay in formalin for 24 hours to be adequately fixed and could become over-fixed as quickly as 36 hours (Mortensen and Brown, 2011). The best methods for antigen retrieval were performed including a wide range of temperatures along with the highly favored sodium citrate buffer at the most recommended pH of 6.0. Although there are more concerns about specificity with polyclonal antibodies, they were used in this study because they are

thought to be less sensitive to fixative issues with formalin (Werner *et al*., 1996). The fixation of the rat abdominal tissues of this study may have irreversibly covered COLI epitopes with cross-bridges and detection of COLI by IHC may not be possible in our sections.

This conclusion that epitope masking is causing problems with specific staining is further supported by the results of the DAB enhancement solution experiment (**Table 13**). Incorporation of imidazole, cobalt chloride, nickel chloride or the enhancer from the DAB kit into the DAB solution have provided intensified staining of tissue sections in multiple other studies (Adams, 1977; Adams, 1981; Utal *et al*., 1998). Their use in our study provided intense staining as well, but did not increase COLI detection. The enhanced DAB solutions made the general morphology of the tissue more detailed in appearance, suggesting the colorimetric substrates were staining tissues as a broad spectrum stain would, with no respect to antigen detection.

The current study examined abdominal incisions of separate groups of rats that were repaired with CollaTape or AlloMax. IHC was used in an attempt to identify COLI in the abdominal wall of rats with CollaTape application. Rat abdominal incisions closed with AlloMax were excised and stained with Masson's Trichrome to compare the separate and combined healing properties of AlloMax, fresh MSCs and PRP. Results from trichrome staining of tissues repaired with CollaTape have previously been reported (Perko, 2012). CollaTape is more properly classified as a wound dressing rather than a surgical mesh and is commonly used in dental procedures to repair oral defects or membrane lacerations (Callan *et al*., 2000; Pikos, 1999). Initially, it was chosen for this study because of its pliable and biodegradable characteristics (Luitaud *et al*., 2007).

Preliminary studies performed by colleagues of this laboratory found that CollaTape would also work as a sufficient vehicle because of its ability to absorb platelet-rich plasma and adhere mesenchymal stromal cells (MSCs), therefore keeping these additives at the wound site (Marie *et al*., 2010; Perko, 2012). AlloMax is a stiff, surgical mesh developed from human dermis and is regularly used for abdominal hernia repair of humans (Bucklen, 2009). The use of AlloMax for human hernia repair is advantageous because it is less flexible than other biodegradable mesh providing increased strength to repaired abdominal walls while also maintaining adequate stretch (Pui *et al*., 2012; Holbrook and Smith, 1993). Orenstein *et al* (2010) found that wounds may heal faster after the application of Allomax, which was attributable to increased cytokine production after AlloMax implantation. AlloMax also outperformed other mesh materials when tested for its ability to adhere MSCs as long as MSCs were incubated overnight with the mesh (Perko, 2012).

Trichrome staining was previously scored for tissues repaired with CollaTape. Slides were produced from excised abdominal tissue of rats at 4 and 8 weeks after receiving an abdominal incision repaired with CollaTape and either PRP alone or in combination with fresh or frozen MSCs. These slides were stained with Masson's Trichrome, photographed and scored by blinded observers using the same scale used in this study (**Table 3**). Although significant differences were not previously found for collagen organization between groups, the group of rats that were repaired with CollaTape, PRP and fresh MSCs had significantly increased amounts of collagen when compared to the healed abdominal wall of rats that were sutured only, or had CollaTape and PRP applied to the repaired wound. It was expected that the amount of collagen

would be increased in this fresh MSC group because tissue from this group also exhibited 100% increased tensile strength when excised at 4 weeks and a 58% increase when excised at 8 weeks (Heffner *et al*., 2012).

The results from scoring the trichrome stained slides for Groups 5, 6, 7, and 8 (Allomax with or without PRP or fresh MSC) found in this study are unexpected due to these previous results. Slides were made from the excised abdominal walls of rats and scored in the same fashion as the groups repaired with CollaTape in the previous study. However, the current study only compared tissues excised at 8 weeks post-operative. The group of rats repaired with AlloMax, PRP and fresh MSCs had the lowest scores for collagen organization and amount. While the organization of collagen continues to be similar between groups, collagen amounts do not mirror relative comparisons of the groups repaired with CollaTape. The group repaired with AlloMax, PRP, and fresh MSCs had the least amount of collagen among groups repaired with AlloMax. Rats that had AlloMax with PRP applied to their abdominal wall exhibited the greatest scores for collagen amount. Although correlation of collagen organization to amount decreased when abdominal walls were repaired with only the AlloMax mesh, an increased positive correlation was found between these 2 collagen characteristics for abdominal wounds that healed for 8 weeks with AlloMax, PRP, and fresh MSCs. Based on this data, even though priming with PRP and fresh MSCs did not significantly increase collagen amount compared to uninjured abdominal wall, it did result is a closer relationship between increases in collagen organization and amount in an abdominal scar ($R^2 = 0.941$). These results cannot be assessed in relation to tensile strength testing because the strength of the AlloMax mesh overwhelmed the results from these tests and the strength of the

abdominal wall itself could not be determined (Heffner *et al*., 2012). It was also a concern that the AlloMax would skew the trichrome scoring results and this is why AlloMax was distinctly outlined if seen in pictures to be scored, and blinded observers were instructed to exclude these areas from influencing their scores of that sample.

Because AlloMax is the only variable between the groups scored previously and in this study, the AlloMax surgical mesh is most likely to blame for differences seen between the 2 studies. As previously mentioned, AlloMax increases cytokine production particularly interleukin-6 (IL-6) (Orenstein *et al*., 2010). Among the many functions of IL-6, it is primarily known for stimulating inflammation (Barrientos *et al*., 2008). MSCs, however, have been shown to secrete anti-inflammatory cytokines (Atoui *et al*., 2008). The MSCs may be working to decrease the inflammation caused by the events related to AlloMax implantation. An inflammatory response is an important component of the wound healing process. The group treated with AlloMax and PRP may have the highest scores for collagen amount and organization because PRP does not manipulate inflammation. In addition, PRP accelerates wound healing by increasing the amount of platelets at the wound site which degranulate and initiate clot formation (Marx, 2004). As described in the introduction, several growth factors are present within the alpha granules from the platelets and their release into the wound site ultimately increases collagen production. In contrast, PRP provides growth factors that are important for MSC survival and function. The use of PRP and fresh MSCs together severely limits AlloMax's healing abilities, as indicated by collagen amount and organization. PRP may be enhancing the production of anti-inflammatory cytokines from MSCs (Atoui *et al*., 2008) counteracting the Allomax effect more than MSCs do alone.

Myocyte degeneration was also scored either previously or currently for excised abdominal tissue of all groups repaired with CollaTape and AlloMax. Myocyte degeneration is thought to not represent breakdown of muscle tissue, but rather the formation of new muscle tissue during wound healing. Scoring of myocyte degeneration was carried out previously for trichrome stained slides of abdominal wall excised from rats implanted with CollaTape alone, CollaTape and PRP, or CollaTape, PRP, and fresh MSCs. The only tissues that had significantly more myocyte degeneration compared to other groups at the same time point were from the 4 week post-operative rats repaired with CollaTape and PRP (Heffner *et al*., 2012). In the current study, scores of trichrome slides were only compared between 8 week post-operative groups. The results show that myocyte degeneration was greatly increased for the group that received AlloMax with PRP. This group also had the greatest abundance of collagen. Increased myocyte degeneration and associated increased collagen amount could indicate, rather than reflecting new muscle formation, that collagen is becoming more integrated into the muscle tissue and replacing areas that were muscle before injury. However, when this theory was tested, myocyte degeneration was found to have an extremely weak correlation to collagen organization or amount in abdominal walls of uninjured, control rats (**Table 15**). From this data, collagen deposition does not appear to have an effect on muscle arrangement. The formation of new muscle after an injury may be primarily due to new myocyte formation during tissue repair. It is also possible that fascia sutured with AlloMax alone may have had the least amount of myocyte degeneration because healing wounds supplemented with this mesh also contain increased levels of IL-8 (Orenstein *et*

al., 2010), which activates matrix metalloproteinase inhibitors, thus decreasing tissue degeneration.

To combat the problems seen with IHC in this study, the best way to go forward is from its beginning. The paraffin-embedded sections used in the current study are likely unable to react to antibodies against collagen because antigens on the tissue are covered with cross-bridges that formed during the fixation procedure. The surgical procedures should be repeated on new Lewis rats and slides could be made from frozen sections. The use of frozen sections would eliminate the suspected problem of formalin over-fixation. IHC of frozen sections would also increase the number of antibodies available for use in this study. Most immediately, the current paraffin-embedded sections could be tested for their sensitivity to antigen retrieval by enzymatic digestion. Proteases have also been successfully used to digest the cross-bridges between epitopes within paraffin-embedded tissue sections. If the cross-bridges are irreversible, antigen retrieval by protease digestion may also be unsuccessful. It is possible that other antibodies will be developed that will work in these tissues or antibodies against other molecules may yield important results using the paraffin-embedded tissue in the future. The detection of COLI in the abdominal wall tissue of rats from this study could clarify our previous results that support the supplementation of fresh MSCs to develop stronger fascia (Heffner *et al*., 2012). The completion of this study would also provide much needed information about abdominal wound healing that could be useful in other hernia related research.

Scoring of trichrome stained slides provided initially unexpected results for abdominal wounds healed with AlloMax and fresh MSCs. The interaction of cytokines

secreted from MSCs and those secreted naturally in response to AlloMax implantation are the suspected reason for these results. To confirm these speculations, immunoassays could analyze the population of cytokines secreted in environments with AlloMax, PRP and fresh MSCs duplicating Groups 5, 6, and 7 of this study. Elucidating the immunologic reaction of MSCs with mesh may also help to predict the effects one could expect to see if the surgical procedures tested here were performed on humans. Currently, a study is in progress to determine the minimal concentration of fresh MSCs needed to provide optimal wound healing. Future studies like these can increase knowledge about MSCs and wound healing. The use of MSCs to increase the strength of healed abdominal wounds by accelerating collagen synthesis was unsuccessful in this study but it may lead to discoveries involving MSC secretions that we were once unaware of. The solution to hernia recurrence is getting closer and further research involving MSCs may discover it.

References:

AbCam. (2010). *Protocols book* (1st ed.). Cambridge, MA.

Albina J, Henry W, Mastrofrancesco B, Martin B, Reichner J. (1995). Macrophage activation by culture in a anoxic environment. *J Immunol*, 155:4391-4396.

Anurov M, Titkova S, Oettinger A. (2012). Biomechanical compatibility of surgical mesh and fascia beign reinforced: dependence of experimental hernia defect repair results on anisotropic surgical mesh positioning. *Hernia*, 16:199-210.

Atoui R, Asenjo J, Duong M, Chen G, Chiu R, Shum-Tim D. (2008). Marrow Stromal Cells as Universal Donor Cells for Myocardial Regenerative Therapy: Their Unique Immune Tolerance. *Ann Thorac Surg*, 85:571-580.

Atwood K and Dako Technical Support Group. (2009). *IHC Staining Methods* (5th ed.). Carpinteria: Dako North America.

Barbul A. (1990). Immune aspects of wound care. *Clin Plast Surg*, 17:433-442.

Barrientos S, Stojadinovic O, Golinko M, Brem H, Tomic-Canic M. (2008). Growth factors and cytokines in wound healing. *Wound Repair Regen*, 16(5):585–601.

Brinchmann J. (2008). Expanding autologous multipotent mesenchymal bone marrow stromal cells. *J Neurol Sci*, 265(1-2):127–130.

Buchwald D, Kaltschmidt C, Haardt H, Laczkovics A, Reber D. (2008). Autologous platelet gel fails to show beneficial effects on wound healing after saphenectomy in CABG patients. *J Extra Corpor Technol*, 40(3):196-202.

Bucklen K. (2009). Recurrent Incisional Hernia Repair and Abdominal Wall Reconstruction with Component Separation Technique using the Bard AlloMax Surgical Graft. *Davol Inc. Clinical Case Report*.

Caldwell R, Holt G, Caprioli R. (2005). Tissue Profiling by MALDI Mass Spectrometry Distinguishes Clinical Grades of Soft Tissue Sarcomas. *Cancer Genomics Proteomics*, 2:33-346.

Callan D, Salkeld S, Scarborough N. (2000). Histologic analysis of implant sites after grafting with demineralized bone matrix putty sheets. *Implant Dent*, 9:36-44.

Carson F. (1997). *Histotechnology: A Self Instructional Text*. Chicago: American Society of Clinical Pathologists Press.

Davol Inc. (2010). *AlloMax* [Brochure]. Warwick, Rhode Island.

DeFrances C and Hall M. (2007). 2005 National Hospital Discharge Survey. *Adv* Data, 385:1-19.

Dent T. (1992). Training, credentialing, and evaluation in laparoscopic surgery. *Surg Clin North Am*, 72(5):1003–1011.

Dickhut A, Pelttari K, Janicki P, Wagner W, Eckstein V, Egermann M, Richter W. (2009). Calcification or dedifferentiation: requirement to lock mesenchymal stem cells in a desired differentiation stage. *J Cell Physiol*, 219(1):219–226.

DuBay A, Choi W, Urbanchek M, Wang X, Adamson B, Dennis R, Kuzon W, Franz M. (2007). Incisional herniation induces decreased abdominal wall compliance via oblique muscle atrophy and fibrosis. *Ann Surg*, 245(1):140–146.

DuBay D, Wang X, Adamson B, Kuzon W, Dennis R, Franz M. (2005). Progressive fascial wound failure impairs subsequent abdominal wall repairs: a new animal model of incisional hernia formation. *Surgery*, 137(4):463–471.

Dufrane D, Mourad M, van Steenberghe M, Goebbels R, Gianello P. (2008). Regeneration of abdominal wall musculofascial defects by a human acellular collagen matrix. *Biomaterials*, 29(14):2237–2248.

Ehrlich H, Krummel T. (1996). Regulation of wound healing from a connective tissue perspective. *Wound Repair Regen*, 4(2):203-210.

Engelhardt E, Toksoy A, Goebeler M, Debus S, Brocker E, Gillitzer R. (1998). Chemokines IL-8, GRO-alpha, MCP-1, IP-10, and Mig are sequentially and differentially expressed during phase-specific infiltration of leukocytes subsets in human wound healing. *Am J Pathol*, 153:1849-1860.

Everts P, Devilee R, Brown Mahoney C, Eeftinck-Schattenkerk M, Box H, Knape J, van Zundert A. (2006). Platelet gel and fibrin sealant reduce allogeneic blood transfusions in total knee arthroplasty. *Acta Anaesthesiol Scand*, 50(5):593-599.

Feng D, Nagy J, Pyne K, Dvorak H, Dvorak A. (1998). Neutrophils emigrate from venules by a transendothelial cell pathway in response to FMLP. *J Exp Med*, 187:903-915.

Franz M, Kuhn M, Wright T, Wachtel T, Robson M. (2000). Use of the wound healing trajectory as an outcome determinant for acute wound healing. *Wound Repair Regen*, 8(6):511–516.

Han S, Yoon T, Lee D, Lee M, Kim W. (2005). Potential of human bone marrow stromal cells to accelerate wound healing in vitro. *Ann Plast Surg*, 55(4):414–419.

Heffner J, Holmes J, Ferrari J, Krontiris-Litowitz J, Marie H, Fagan D, Perko J, Dorion H. (2012). Bone marrow-derived mesenchymal stromal cells and platelet-rich plasma on a collagen matrix to improve fascial healing. *Hernia*, in press.

Holbrook K and Smith C. (1993). *Connective Tissue and Its Heritable Disorders*. New York: Wiley-Liss.

Horwitz E, Le Blanc K, Dominici M, Mueller I, Slaper-Cortenbach I, Marini F, Deans R, Krause D, Keating A, International Society for Cellular Therapy. (2005). Clarification of

the nomenclature for MSC: The international society for cellular therapy position statement. *Cytotherapy*, 7(5):393–395.

Javazon E, Colter D, Schwarz E, Prockop D. (2001). Rat marrow stromal cells are more sensitive to plating density and expand more rapidly from single-cell-derived colonies than human marrow stromal cells. *Stem Cells*, 19(3):219–225.

Junqueira L, Carneiro J, Kelley R. (1992). *Basic Histology* (7th ed.). East Norwalk: Appleton and Lange.

Kambic H, Reyes E, Manning T, Waters K, Reger S. (1993). Influence of AC and DC electrical stimulation on wound healing in pigs: a biomechanical analysis. *J Invest Surg*, 6(6):535–543.

Klinge U, Si Z, Zheng H, Schumpelick V, Bhardwaj R, Klosterhalfen B. (2001). Collagen I/III and matrix metalloproteinases (MMP) 1 and 13 in the fascia of patients with incisional hernias. *J Invest Surg*, 14(1):47–54.

Kobayashi S, Nakano M, Kimura T, Schaap A. (1987). On the mechanism of the peroxidase-catalyzed oxygen-transfer reaction. *Biochemistry*, 26(16):5019-5022.

Lang R, Patel D, Morris J, Rutschman R, Murray P. Shaping gene expression in activated and resting primary macrophages by IL-10. *J Immunol*, 169:2253-2263.

Leong A and Leong T. (2011). Standardization in Immunohistology. *Methods Mol Biol*, 724:37-68.

Li C, Ziesmer S, Lazcano-Villareal O. (1987). Use of Azide and Hydrogen Peroxide as an Inhibitor for Endogenous Peroxidase in the Immunoperoxidase Method. *J Histochem Cytochem*, 35(12):1457-1460.

Luitaud C, Laflamme C, Semlali A, Saidi S, Grenier G, Zakrzewski A, Rouabhia M. (2007). Development of an engineering autologous palatal mucosa-like tissue for potential clinical applications. *J Biomed Mater Res B Appl Biomater*, 83(2):554-561.

Madden J and Peacock E. (1971). Studies on the biology of collagen during wound healing: 3. dynamic metabolism of scar collagen and remodeling of dermal wounds. *Ann Surg*, 174(3):511–520.

Marie H, Zhang Y, Heffner J, Dorion H, Fagan D. (2010). Biomechanical and Elastographic Analysis of Mesenchymal Stromal Cell Treated tissue Following Surgery. *J Biomech* Eng, 132(7):074503.

Marshall J. (2004). Mast-cell response to pathogens. *Nat Rev Immunol*, 4:787-799.

Marx R. (2004). Platelet-rich plasma: evidence to support its use. *J Oral Maxillofac Surg*, 62(4):489-496.

McCulloch J and Kloth L. (2010). *Wound Healing: Evidence Based Management* (4th ed.). Philadelphia: F.A. Davis.

McFarlin K, Gao X, Liu Y, Dulchavsky D, Kwon D, Arbab A, Bansal M, Li Y, Chopp M, Dulchavsky S, Gautam S. (2006). Bone marrow-derived mesenchymal stromal cells accelerate wound healing in the rat. *Wound Repair Regen*, 14(4):471–478.

Miller R. Technical Immunohistochemistry: Achieving Reliability and Reproducibility of Immunostains. *Society for Applied Immunohistochemistry 2001 Annual Meeting*.

Minguell J, Conget P, Erices A. (2000). Biology and clinical utilization of mesenchymal progenitor cells. *Braz J Med Biol Res*, 33(8):881–887.

Mortensen E and Brown J. (2003). Effects of fixation on tissues. *Methods Mol Med*, 81:163-179.

Oreffo R, Cooper C, Mason C, Clements M. (2005). Mesenchymal stem cells: lineage, plasticity, and skeletal therapeutic potential. *Stem Cell Rev*, 1(2):169–178.

Orenstein S, Qiao Y, Kaur M, Kluch U, Kreutzer D, Novitsky Y. (2010). Human monocyte activation by biologic and biodegradable meshes in vitro. *Surg Endosc*, 24:805-811.

Ortonne J, Loning T, Schmitt D, Thivolet J. (1981). Immunomorphological and ultrastructural aspects of keratinocyte migration in epidermal wound healing. *Virchows Arch A Pathol Anat Histol*, 392(2):217-230.

Peacock E. (1984). *Wound Repair* (3rd ed.). Philadelphia: Saunders.

Perko J. (2012). Mesenchymal stromal cells and platelet-rich plasma on a collagen matrix to improve fascial repair. (Graduate thesis). Retrieved from etd.ohiolink.edu.

Pikos M. (1999). Maxillary sinus membrane repair: report of a technique for large perforations. *Implant Dent*, 8:29-34.

Pui C, Tang M, Annor A, Ebersole G, Frisella M, Matthews B, Deeken C. (2012). Effect of repetitive loading on the mechanical properties of biological scaffold materials. *J Am Coll Surg*, 215(2):216-228.

Ruggeri Z. (2002). Platelets in Atherothrombosis. *Nat Med* 8:1227-1234.

Saratzis N, Saratzis A, Melas N, Kiskinis D. (2008). Non-activated autologous platelet-rich plasma for the prevention of inguinal wound-related complications after endovascular repair of abdominal aortic aneurysms. *J Extra Corpor Technol*, 40(1):52-56.

Smith P, Kuhn M, Franz M, Wachtel T, Wright T, Robson M. (2000). Initiating the inflammatory phase of incisional healing prior to tissue injury. *J Surg Res*, 92(1):11–17.

Strodtbeck F. (2001). Physiology of wound healing. *Newborn Infant Nurs Revs*, 1(1):43–52.

Tomasek J, Gabbiani G, Hinz B, Chaponnier C, Brown R. (2002). Myofibroblasts and mechanoregulation of connective tissue remodeling. *Nat Rev Mol Cell Biol*, 3(5):349-363.

True L. (2008). Quality control in molecular immunohistochemistry. *Histochem Cell Biol*, 130:473-480.

Tyrone J, Marcus J, Bonomo S, Mogford J, Xia Y, Mustoe T. (2000). Transforming growth factor beta3 promotes fascial wound healing in a new animal model. *Arch Surg*, 135(10):1154-1159.

Vaalamo M, Mattila L, Johansson N, Kariniemi A, Karjalainen-Lindesberg M, Kahari V, Saarialho-Kere U. (1997). Distinct populations of stromal cells express collagenases-3 (MMP-13) and collagenase-1 (MMP-1) in chronic ulcers but not in normally healing wounds. *J Invest Dermatol*, 109:96-101.

Wagner W and Ho A. (2007). Mesenchymal stem cell preparations–comparing apples and oranges. *Stem Cell Rev*, 3(4):239–248.

Wahl S. (1985). Host immune factors regulating fibrosis. *Ciba Found Symp*, 114:175-195.

Weisel J, Francis C, Nagaswami C, Marder V. (1993). Determination of the topology of factor XIIIa-induced fibrin gamma-chain cross-linksby electron microscopy of ligated fragments. *J Biol Chem*, 268:26618-26624.

Werner M, von Wasielewski R, Komminoth P. (1996). Antigen retrieval, signal amplification and intensification in immunohistochemistry. *Histochem Cell Biol*, 105:253-260.

White B, Osier C, Gletsu N, Jeansonne L, Baghai M, Sherman M, Smith C, Ramshaw B, Lin E. (2007). Abnormal primary tissue collagen composition in the skin of recurrent incisional hernia patients. *Am Surg*, 73(12):1254–1258.

Wu Y, Wang J, Scott P, Tredget E. (2007). Bone marrow-derived stem cells in wound healing: a review. *Wound Repair Regen*, 15 Suppl 1:S18-S26.

Yan H and Yu C. (2007). Repair of Full-Thickness Cartilage Defects with Cells of Different Origin in a Rabbit Model. Arthroscopy, 23(2):178-187.

Zieren J, Castenholz E, Baumgart E, Müller J. (1999). Effects of fibrin glue and growth factors released from platelets on abdominal hernia repair with a resorbable PGA mesh: experimental study. *J Surg Res*, 85(2):267–272.